Public Interest Energy Research (PIER) Program

White Paper

FIRE AND CLIMATE CHANGE IN CALIFORNIA

Changes in the Distribution and Frequency of Fire in Climates of the Future and Recent Past (1911–2099)

A White Paper from the California Energy Commission's California Climate Change Center

Prepared for: California Energy Commission

Prepared by: Simon Fraser University and University of California, Berkeley

JULY 2012

CEC-500-2012-026

Meg Krawchuk

Max Moritz

Simon Fraser University and
University of California, Berkeley

ACKNOWLEDGEMENTS

Alan and Lorraine Flint of the United States Geological Survey, along with Jim Thorne and Ryan Boynton from the University of California, Davis, provided downscaling and hydrologic modeling of climate data for this project. Jim Thorne and Jackie Bjorkman provided urban growth scenarios from the UPlan model. Thank you to two anonymous reviewers who greatly improved the manuscript.

PREFACE

The California Energy Commission's Public Interest Energy Research (PIER) Program supports public interest energy research and development that will help improve the quality of life in California by bringing environmentally safe, affordable, and reliable energy services and products to the marketplace.

The PIER Program conducts public interest research, development, and demonstration (RD&D) projects to benefit California. The PIER Program strives to conduct the most promising public interest energy research by partnering with RD&D entities, including individuals, businesses, utilities, and public or private research institutions.

PIER funding efforts are focused on the following RD&D program areas:

- Buildings End-Use Energy Efficiency
- Energy Innovations Small Grants
- Energy-Related Environmental Research
- Energy Systems Integration
- Environmentally Preferred Advanced Generation
- Industrial/Agricultural/Water End-Use Energy Efficiency
- Renewable Energy Technologies
- Transportation

In 2003, the California Energy Commission's PIER Program established the California Climate Change Center to document climate change research relevant to the states. This center is a virtual organization with core research activities at Scripps Institution of Oceanography and the University of California, Berkeley, complemented by efforts at other research institutions.

For more information on the PIER Program, please visit the Energy Commission's website http://www.energy.ca.gov/research/index.html or contract the Energy Commission at (916) 327-1551.

ABSTRACT

We examine a macro-scaled perspective of fire and climate for California and highlight landscapes where sensitivity and exposure to climate change has the potential to induce alteration of future fire activity. This research presents just one method of proposing a future of fire and includes many caveats and assumptions. Using statistical models, we relate the probability of burning in 1080-m landscapes over a 30-year baseline period of 1971–2000 to climate variables for the same period. These climate variables aim to represent spatial variation in vegetation growth conditions and the seasonal dryness necessary for burning. A metric of distance to human development is used to examine human influence on fire activity via ignition and/or suppression. We quantify how the risk of relatively long-term tendency for burning might change with climate over the next 100 years based on projections from two Global Climate Models and two emissions scenarios. Model outcomes suggest varying degrees of increased future fire activity in more productive regions of California however by 2070–2099, the two GCMs selected for the study disagree in the polarity in response for drier, less productive regions.

The second component of this study is retrospective. We test the temporal transferability of baseline models by back-casting using 1971–2000 model parameters but incorporating climate and development data from 1941–1970. These baseline back-casts were compared against model outcomes developed using data from the 30-year period from 1941–1970. Though fire records from before 1950 were not kept as reliably as in more recent periods, this method helps to understand how well projections of future fire might reflect actual future events. Baseline models are then also used with observed climate records for periods 1911–1940, which allows us to consider differences among future projections of fire and climate in the context of the range estimated for the last century.

Keywords: California Energy Commission, fire, climate change, hydrologic models, future projections, historic transferability, probability of burning, fire return interval

Please use the following citation for this paper:

Krawchuk, M. A., and M. A. Moritz (Simon Fraser University; University of California, Berkeley). 2012. ***Fire and Climate Change in California.*** California Energy Commission. Publication number: CEC-500-2012-026.

TABLE OF CONTENTS

Acknowledgements ..... **i**
PREFACE ..... **ii**
ABSTRACT ..... **iii**
TABLE OF CONTENTS ..... **iv**
Section 1: Fire and Future Climate Change in California **1**
1.1 Introduction 1
1.2 Methods 3
1.2.1 Overview 3
1.2.2 Data 4
1.2.3 Statistical Modelling 15
1.3 Results 20
1.3.1 Model Assessment and Validation 20
1.3.2 Current and Future Fire 22
1.3.3 Mean Fire Return Intervals, mFRI 23
1.4 Discussion 23
Section 2: Fire and Past Climates in California: Back-Casting through the Century **37**
2.1 Introduction 37
2.2 Methods 38
2.2.1 Fire Data 38
2.2.2 Climate Data 38
2.2.4 Land Cover Data 39
2.2.5 Statistical Modelling 40
2.2.6 Model Back-Casts 40
2.3 Results and Discussion 40
2.3.1 Model Transferability 40
2.3.2 Historical Back-Casts of Fire and Climate in the Context of Future Projections 41
References 47
Glossary 50

LIST OF FIGURES

Figure 1: Jepson Ecoregions within the State of California, in the Western United States 4

Figure 2: Frequency of Burning in 1080 m Landscapes across California in Two Different Time Periods, Based on FRAP Data. (a) The entire burned area dataset from FRAP records dating from 1878 to 2009. (b) Fire data from the shorter, 30-year period 1971–2000, used for model development. Note that numerous landscapes have burned more than once, especially in southwestern California 6

Figure 3: Processing Steps of Fire Polygons (Fires) to Fire Frequency Resulted in Simplification of the Raw FRAP Data, Including the Removal of Many Small Fires Due to Landscape Sampling Size and Processing Algorithms 8

Figure 4: The Mosaic of Unburned and Burned Patches of Chaparral Is Still Visible One Year After the 2007 Zaca Fire Outside of Santa Barbara, California. The sampling resolution of 1080 m simplifies these finer resolution patterns of burning. Fire burns with varying intensity resulting in heterogeneous severity within the perimeter recorded by the FRAP polygons. These patterns of severity are lost in our models of landscape burning, but are important to remember, since they contribute to post-fire structure and function of the ecosystem. 8

Figure 5: Changes in the Distribution of Annual Precipitation for 2010–2039 in the PCM (a) and GFDL (b) GCMs (Hatched) against Recent Historical 1971–2000 Conditions (Blue), and Changes for 2070–2099 for the PCM (c) and GFDL (d). Both GCMs project a warmer future for California, but the PCM projects warmer conditions with relatively modest increases in precipitation and the GFDL projects warmer-drier conditions. These differences are most obvious in the 2070–2099 data. 10

Figure 6: The Placement of GFDL and PCM GCMs within an Ensemble of 16 GCMs from the CMIP3 Archive. Note these are statewide annual mean temperatures and annual precipitation, masking much regional heterogeneity 11

Figure 7: (a) Distance to Development Metric (D_dev) Generated from UPlan Data and Used for 1971–2000 Models, (b) Distance to Development Based on the UPlan Smart Growth Scenario, and (c) from the UPlan Base Case, Business-as-Usual Growth Scenario. Areas of water are shown in white, with the exception of islands that have been left blank, since our D_dev metric is somewhat arbitrary for them. 14

Figure 8: Spatial Patterns in Explanatory Climate Variables for 1971–2000. (a) Maximum monthly temperature, (b) seasonality in precipitation, (c) seasonality in potential evapotranspiration, (d) seasonality in actual evapotranspiration, and (e) annual climatic water deficit. 19

Figure 9: Exemplar Shapes of Quadratic Relationships for (a) Maximum Monthly Temperature, and (b) Seasonality in Actual Evapotranspiration, from One of the Ten Models 21

Figure 10: Assessment of Zero-inflated Poisson Models Using the Difference between the Probabilities of Predicted and Observed Counts for Each of the Ten Sub-models 22

Figure 11: (a) Probability of Burning at Least Once under 1971–2000 Conditions, (b) Change in Probability by 2010–2039, and (c) Projected Future Probability over Thirty Years for 2010–2039 Based on the "Warmer-Drier" GFDL GCM, A2 Emission Scenario and UPlan Base Case Urban Growth. (c–d) projections using the "Warmer-Wetter" PCM GCM. Areas of water, agriculture, and urban infrastructure are masked in white, with the exception of low-density residential housing (see Methods). 27

Figure 12: (a) Probability of Burning Two or More Times under 1971–2000 Conditions, (b) Change in Probability by 2010–2039, and (c) Projected Future Probability of Burning Two or More Times for 2010–2039 Based on the GFDL GCM, A2 Emission Scenario and UPlan Base Case Urban Growth, and (d–f) Projections Using the PCM GCM. Areas of water, agriculture, and urban infrastructure are masked in white, with the exception of low-density residential housing (see Methods). 28

Figure 13: (a) Probability of Burning at Least Once under 1971–2000 Conditions, (b) Change in Probability by 2070–2099, and (c) Projected Future Probability of Burning at Least Once over Thirty Years for 2070–2099 Based on the GFDL GCM, A2 Emission Scenario and UPlan Base Case Urban Growth. (d–f) projections using the PCM GCM. Areas of water, agriculture, and urban infrastructure are masked in white, with the exception of low-density residential housing (see Methods)..... 29

Figure 14: (a) Probability of Burning Two or More Times under 1971–2000 Conditions, (b) Change in Probability by 2070–2099, and (c) Projected Future Probability of Burning Two or More Times for 2070–2099 Based on the GFDL GCM, A2 Emission Scenario and UPlan Base Case Urban Growth. (d–f) projections using the PCM GCM. Areas of water, agriculture, and urban infrastructure are masked in white, with the exception of low-density residential housing (see Methods)..... 30

Figure 15: Agreement in Decreased and Increased Projected Changes in at Least One Fire (a,b) and Disagreement (c) for 2010–2039, and 2070–2099 (d–f). Areas of water, agriculture, and urban infrastructure are masked in light grey, with the exception of low-density residential housing (see Methods)..... 31

Figure 16: Mean Fire Return Interval (mFRI, 30 ÷ Expected Number of Fires) for 1971–2000 and 2010–2039 for (a,b) GFDL and (c,d) PCM GCMs. Urban, agricultural, and water are masked in grey..... 32

Figure 17: Mean Fire Return Interval (mFRI, 30 ÷ Expected Number of Fires) for 1971–2000 and 2070–2099 for (a,b) GFDL and (c,d) PCM GCMs. Urban, agricultural, and water are masked in grey..... 33

Figure 18: Box and Whisker Plots of Mean Fire Return Interval, mFRI for 1971–2000, 2010–2039, and 2070–2099 Based on GFDL and PCM GCMs for Six Types of Wildlife Habitat Relationship (WHR), (a) Chamise-redshank, (b) Blue oak, (c) Mixed chaparral, (d) Douglas fir, (e) Redwood, and (f) Pinyon-juniper. Note, outliers are not shown. The spatial distribution of each WHR is shown alongside the distributions of return interval. 36

Figure 19: Frequency of Burning in 1080-m Landscapes over 30-year Periods across California in Different Time Intervals, Based on FRAP Data. (a) 1911–1940, (b) 1941–1970, (c) 1971–2000. Note

the relative sparseness of data recorded for the 1911–1940 period, reflecting differences in recording. 39

Figure 20: Probability of Burning at Least Once in (a) 1971–2000, (b) the Delta, and (c) the Baseline Back-cast Estimate for 1941–1970 Using 1971–2000 Model Parameters. Delta values represent the baseline 1971–2000 minus the back-cast so that the negative values, indicated by yellow, indicate more fire and positive values, indicated by blue, indicate less fire. Areas in white are masks for development, agriculture, and water. 42

Figure 21: Comparison of Models for Landscapes Burning at Least Once (a) Baseline Back-cast Built with 1971–2000 Data, to (b) 1941–1970 Estimates Built with 1941–1970 Fire Data. Areas in white are masks for development, agriculture, and water. 43

Figure 22: (a) Differences Between 1941–1970 Estimates and Baseline Back-casts. Yellow/orange indicates areas where more fire was predicted by baseline back-casts than in 1941–1970 estimates, blues indicate the reverse. Values are masked to highlight areas of most difference. For (a) the white mask covers areas of little difference, values +/- 0.025. For (b) since general under-reporting might have resulted in an overall diminished probability of fire in the 1941–1970 estimates, the same data are shown but with an additional mask for values up to -0.05. The result highlights key areas of difference between baseline back-casts and 1941–1970 estimates. Areas of agriculture, water, and development at 1941–1970 are also masked in white. 44

Figure 23: Probability of Burning at Least Once in (a) 1971-2000, (b) the Delta Showing a Subtraction of 1971–2000 Minus 1911–1940 Values, and (c) the Back-cast Estimate for 1911–1940 Based on Baseline 1971–2000 Model Parameters. Areas in white are masks for agriculture (based on 1971–2000 data), development, and water. Note the marked reduction of the development footprint in the southwest. 45

Figure 24: Expected Mean Fire Return Interval (mFRI) for (a) 1911–1940, (b) 1941–1970, (c) 1971–2000, (d,e) 2010–2039 (GFDL then PCM), (f,g) 2070–2099 (GFDL then PCM) Based on 1971–2000 Model Parameters, with no Mask for Agriculture or Development. Water bodies are masked in white. 46

LIST OF TABLES

Table 1: Explanatory Variables Used in Statistical Models. All climate variables were quantified as a 30-year climatology for 1971 to 2000. 17

Table 2: Model Assessment and Validation 21

Unless otherwise noted, all tables and figures are provided by the author.

Section 1: Fire and Future Climate Change in California

1.1 Introduction

Climate change through the twenty-first century is anticipated to alter patterns of fire activity globally, however our understanding of spatial variability in these disruptions and the potential magnitude of response is far from complete. There are documented changes in fire and climate over long time horizons with periods of warming, pluvials, coolings, and drought generating different fire signatures (Marlon et al. 2008; Power et al. 2008; Swetnam and Betancourt 1990), alongside evidence that humans have contributed to patterns of fire activity at some spatial and temporal scales (Fulé et al. 2011; Whitlock et al. 2010; Marlon et al. 2008). While the degree of influence by biophysical and eco-cultural controls over fire are far from clear, our basic understanding of the relationships between fire and climate suggest that burning over the next century may be altered due to three general factors:

1. Direct effects of changes in fire conditions such as drought, high temperatures, winds, and their seasonality
2. An indirect effect on fire through vegetation—that is, by climate altering the structure and abundance of biomass to burn
3. Through changes in ignition potential due to shifting spatial or temporal patterns of lightning and human behavior in response to factors such as climate policy and environmental management.

Though manifested in different ways, much of the anticipated change in global fire activity will derive from altered patterns of temperature and precipitation (Pechony and Shindell 2010; Krawchuk et al. 2009; Scholze et al. 2006).

In California, years of higher temperatures and less precipitation are thought to have increased recent historical fire activity in some regions, but not all (Westerling et al. 2006). This spatially varying relationship is complex, but the rationale is not necessarily complicated. Consider that there are vast areas of forested lands where resources to burn, defined here as vegetation, are readily available, and we might expect rising temperatures and reduced precipitation to result in more fire due to drying of these abundant fuels. This situation is commonly referred to as a *fire weather-* or *conditions-limited system.*

Contrast this situation to landscapes with less, and sparse, vegetation that might incur less fire under a higher-temperature, less-precipitation scenario because the growth of vegetation would diminish with moisture stress, resulting in insufficient fuels to carry a fire, regardless of prime fire weather conditions. This situation is referred to as a *fuel-* or *resource-limited system.*

Wetter years might flip this contrast, to give more fire in resource-limited areas as high productivity generated by wet growing season conditions would provide a pulse of biomass that would cure to fuel for burning during the dry season of the year(s) that followed. Such

resource-limited and conditions-limited systems are book-ends, with a vast heterogeneity in response occurring in between (Krawchuk and Moritz 2011; Meyn et al. 2007).

Spatial and temporal heterogeneity in burning, whether in conditions- or resources-limited areas, is a form of selection, where fire preferentially burns in, or consumes, some areas over others as a function of its requirements for resources to burn, atmospheric conditions for burning, and an ignition agent. Johnson (1980), in discussing the selection of habitat by animals, describes an ordering of processes, and this ordering is also useful in considering scales used in the study of fire. According to Johnson (1980), first-order selection can be defined as the long-term geographic range of a species; second-order as the home range of an individual or social group; third-order as the use of a suite of elements within a home range; and fourth-order as the particular items used at a site.

Much work on fire has focused on the second- to fourth-order elements of where fire occurs and why—as combustion and fire behavior and patterns in fire size and annual area burned. For example, work on fire and future climate change across California by Westerling et al. (2011) and Westerling and Bryant (2008) quantifies patterns in monthly area burned as a function of temporally explicit antecedent and contemporaneous conditions, and Littell et al. (2009) look at patterns of burning at an annual resolution. More specifically, Littell et al. (2009) looked at annual area burned within ecoprovinces across the western United States, including most of California, and considered conditions at the time of a particular fire year or fire season, and lagged periods leading up to them. In contrast, ideas developed by Parisien and Moritz (2009) and Krawchuk et al. (2009) consider first-order selection by fire: what controls broad scale distribution in the probability of burning at decadal to multidecadal scales, and what is the climate space in which fire thrives? This latter approach focuses on understanding the broad geographic distribution of fire as a function of environmental factors representing resources and conditions for burning, quantified at a climatological resolution: a *pyrogeography.* This macro-scaled approach takes a step back from asking questions about the finer details of fire behavior and monthly/annual occurrence and focuses on longer-termed patterns.

Here, we develop the macro-scaled perspective of fire for California and examine the vulnerability of landscapes to climate change-induced alteration of fire activity. Burning can take on many characteristics, including seasonality, intensity, type, size, and frequency; our focus for this work is frequency of fire. Using statistical models, we relate the probability of a 1080 meter (m) landscape burning over a 30-year period (1971–2000) to climate variables for the same period that represent spatial variation in vegetation growth conditions, and the seasonal dryness necessary for fires to burn. A metric of distance to human development is used as a proxy of human influence via ignition and/or suppression. We then examine how this relatively long-term tendency for burning might change over the next 100 years with climate based on projections from two global climate models (GCMs). One GCM, NOAA's GFDL CM2.1, simulates warmer and much drier conditions and the other, NCAR's PCM, a warmer and relatively wetter scenario with less change in temperature and little overall change in precipitation. Future projections of human development are included and represented by simulated outcomes of the UPlan model (Walker et al. 2007).

We look at three general components of future fire: (a) using the current and potential future probabilities of landscape fire occurrence, we calculate the difference between them - the delta, as a spatially explicit metric of change; (b) we compare projected changes between the two GCMs to identify areas of disagreement; and (c) since the number of fires per study cell were

calculated for 30-year periods, we use the inverse of fire counts to represent a fire return interval. The return interval metric is used to explore projected changes within the distribution of six Wildlife Habitat Relationship types (WHR)[1] to propose how future climate and development might affect fire regimes for Chamise-redshank, Blue oak, Mixed chaparral, Douglas fir, Redwood, and Pinyon-juniper distributions.

This research presents one method of proposing a future of fire, using simulated future climate data from only two GCMs. The work includes many caveats and assumptions associated with the fire data, metrics of human development, future climate, statistical modeling, spatial and temporal scales, transient change in fire regimes, and analogues. We describe many of these caveats and assumptions within the document. Readers will likely identify additional limitations including items they would have handled in different ways. We by no means suggest the methods and results of this research to be paramount; however, we offer them as a rigorous and thoughtful examination of potential risks to altered fire activity in California posed by future climate change.

1.2 Methods

1.2.1 Overview

The study region covers the State of California, an area of approximately 400 000 square kilometers (km^2), or 100 million acres (Figure 1). Fire is common in California because of the seasonality in climate, but also because of people. In the Southwest and Central Coast Jepson ecoregions (Figure 1) of the State, winter wet/summer dry, Mediterranean-type seasonality and relatively warm annual temperatures result in pulses of vegetation growth followed by drying that are ideal for fire and attractive to people. The Sierra Nevada, Northwest, and Cascades ecoregions are heavily forested and support more scattered human populations. The Central Valley is largely agricultural and human-dominated. The Modoc ecoregion has sparse populations within a dry, colder continental climate that supports a mixture of sagebrush and forested areas. In the southeast, the arid Sonoran and Mohave deserts support relatively little vegetation to burn, and east of Sierra Nevada is also relatively dry due to a rainshadow effect.

We developed statistical models of recent historical burning across the State at a spatial resolution of 1080 m (hereafter referred to as a *landscape;* roughly 116 hectares or 288 acres) and temporal resolution of 30 years (1971–2000) representing the general distribution and abundance of recent fire (Figure 2). A sparse sampling method was used to diminish the likelihood of over-fitting models to the data. We used zero-inflated Poisson regression models (Zuur 2009) to quantify the relationship between the number of times a landscape burned during the 30-year sampling interval and associated climate characteristics representing resources and conditions for fire. These models allowed us to estimate the probability of burning at least once within a 30-year interval, as well as identifying areas burning multiple times. We included a metric of distance to human development to quantify the additional role human access might play in describing patterns of burning. The lack of future projections for lightning precluded its use in models as an explicit ignition agent, though historical lightning climatologies are available for the region.

---

[1] California Fish and Game. Wildlife Habitats — California Wildlife Habitat Relationships System. http://www.dfg.ca.gov/biogeodata/cwhr/wildlife_habitats.asp.

Parameters from the statistical models were combined with projections of future climate from two GCMs using two emissions scenarios to determine how fire activity might change under future climates. One of the GCMs simulates a generally warmer-drier future climate for California; whereas, the other simulates a warmer future with little change in precipitation; we refer to these as warmer-drier and warmer-wetter, respectively. Details of these two models, their selection, and placement within a broader 16 GCM model ensemble are described in 1.2. 2.2 Climate Data. We also included projections from the UPlan urban growth model to quantify projected future distances to human development that might affect fire activity, and mask areas where urban growth might remove resources for burning.

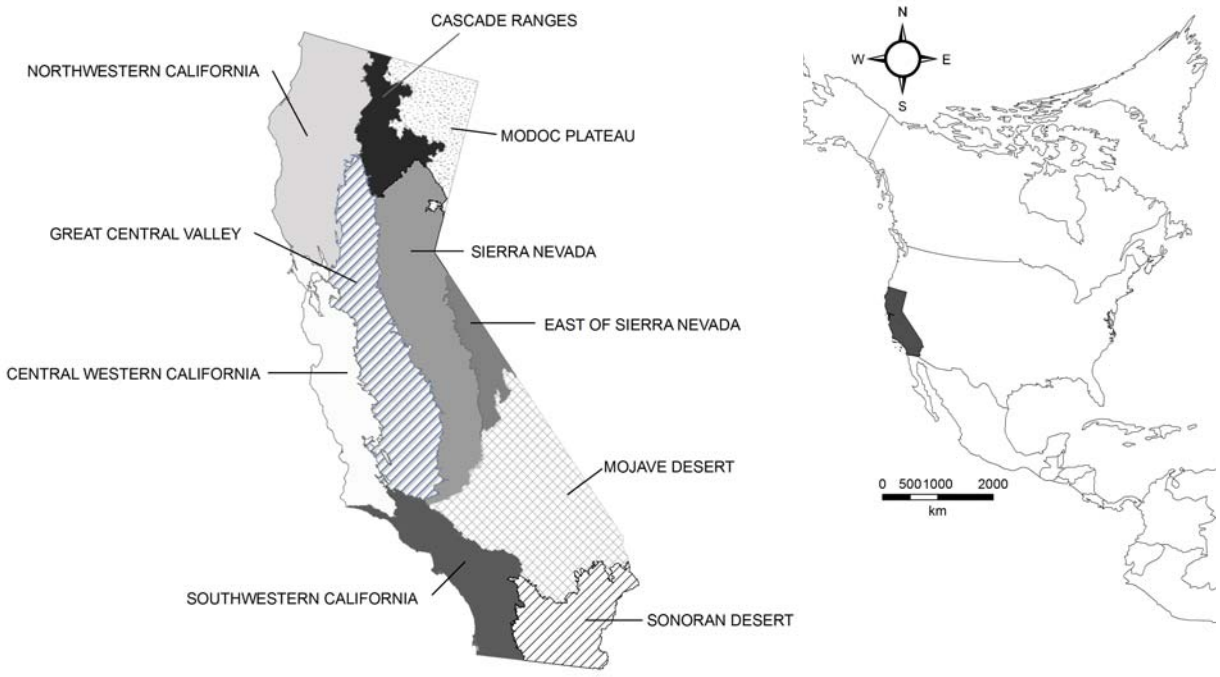

Figure 1: Jepson Ecoregions within the State of California, in the Western United States

1.2.2 Data

1.2.2.1 Fire Data

Data from the California Department of Forestry (CAL FIRE) and Fire Protection Fire and Resource Assessment Program (FRAP) fire polygon dataset[2] were used for statistical models. We extracted data from 1971–2000 to develop models of the recent historical distribution of fire based on fire frequency within 1080 m sampling cells that we refer to as landscapes. We also examined data from 1941–1970 to explore the temporal transferability of 1971–2000 models; this work is presented in Section 2. The 30-year windows of fire were specifically selected to match climate data for that same period.

[2] CDF/FRAP. Data. http://frap.fire.ca.gov/data/frapgisdata/select.asp.

There are many caveats that accompany the fire data, associated with fire sizes recorded and temporal consistency. The FRAP online documentation accompanying the fire polygon database highlights that these data assemble the most complete record of fire in California, and notes that it is a reasonable view of past large fires, but is not fully complete. The data are available from 1878–2010, with a focus on more comprehensive assembly of data from 1950 onward. The database we used was published in early 2010 and included fires up to 2009. Data are contributed from multiple sources, including CAL FIRE (CDF), the United States Department of Agriculture (USDA) Forest Service Region 5, Bureau of Land Management (BLM), National Park Service, Contract Counties, and other agencies. Whenever possible, data are solicited from the Bureau of Indian Affairs and Department of Defense.

The threshold size of fires included in the database varies, but in general, large fires are recorded and small ones are not. As a rule of thumb, Forest Service and Park Service data include fires 10 acres and larger, CAL FIRE data includes those 300 acres and larger for the period we used to characterize recent historical fire. Our study landscapes cover an area of 288 acres, roughly matching the CAL FIRE cut-off.

The Forest Service has contributed data back to 1878 and Park Service back to 1921, and CAL FIRE considers their records complete back to 1950. The summary included with the fire data indicates that BLM has not contributed fires prior to 2002; however, the fire database shows 245 fires under BLM jurisdiction for the 1971–2000 study period, totaling 188,788 acres (76,400 hectares, ha), mostly in central, western, and northern parts of the state. Though others have suggested the necessity to mask out BLM lands due to lack of data contribution, mapping exercises show much of the BLM land falls within sparsely vegetated Mojave and Sonoran deserts, where examination of FRAP in nearby Forest Service and Park Service land also shows no evidence of fire; this despite the long-standing contribution of fire records by Forest and Park Service to the FRAP. We interpret this evidence as sufficient to include the BLM areas of California in our study; however, models may be underestimating fire in drier parts of the state. The inclusion of BLM lands provides interesting biophysical contrast to these regional analyses.

Numerous processing steps were necessary to translate FRAP fire polygons to a surface quantifying the number of times each landscape burned in the 1971–2000 period. Data from 1971–2000 were extracted from the full FRAP fire polygon dataset. We screened data to remove obvious duplicate records. No lower threshold of fire size was used because data processing, described below, removed the majority of small fires from the data set. In ArcInfo, polygons were overlapped, and the frequency of burning was calculated using the REGIONPOLYCOUNT command. A raster surface of the number of times burned from 1971–2000 was generated at a 1080 m resolution (Figure 2b) based on the value found at each landscape's centre. The sum of all burn counts at this 1080 m resolution accounted for 92 percent of area burned calculated from the FRAP database.

a) 1878 to 2009 b) 1971 to 2000

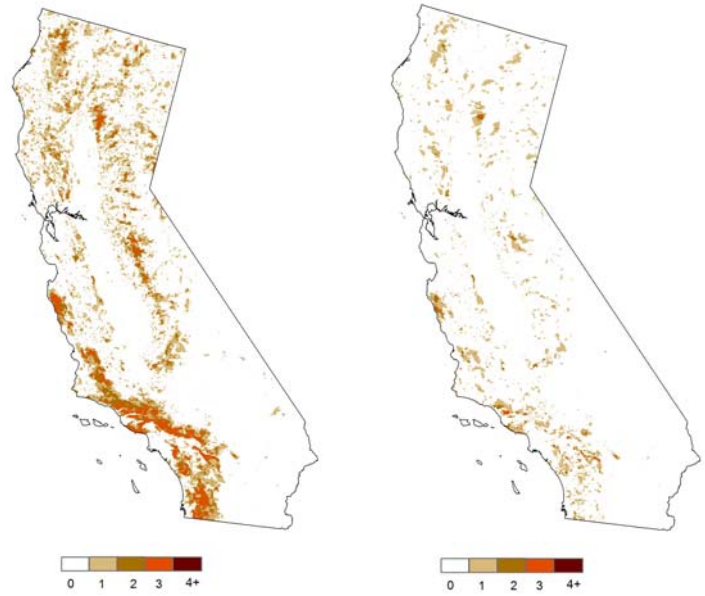

Figure 2: Frequency of Burning in 1080 m Landscapes across California in Two Different Time Periods, Based on FRAP Data. (a) The entire burned area dataset from FRAP records dating from 1878 to 2009. (b) Fire data from the shorter, 30-year period 1971–2000, used for model development. Note that numerous landscapes have burned more than once, especially in southwestern California

The selection of the landscape resolution, absence of a lower size threshold for inclusion of fire data, and the use of the landscape centre for converting burn polygons to a raster surface for statistical analyses all contribute critical decisions in the translation of fire data to fire frequency product. For example, the use of the landscape centre for polygon-to-raster conversion resulted in a majority of small fires being removed from the dataset (Figure 3); fires only slightly less than the landscape, 288 acres (116 ha), were retained. Mapping errors and generalizations are common throughout the raw data provided by the FRAP fire data, and we suggest the method we employed for including fire data holds logic given the uncertainty in the data and processing tools.

The fire frequency data product contains a large number of zeroes. Of the resulting 262,704 landscapes, 239,986 (91 percent) incurred no fire in the 30-year study interval, 20,184 incurred one fire, 2,063 incurred two, 384 incurred three, and 105 incurred four or more. The cell size for analyses was selected as a balance between the desire to examine finer-scaled topographic and landscape patterns in probability of burning with spatial limitations of the fire data provided by FRAP. This study makes the assumption that by using a relatively coarse, 30-year sample resolution with the intermediate-scaled spatial resolution, we step away from explicitly incorporating metrics such as "time since last fire" in our model structure. We assume that adequate regrowth of vegetation for subsequent burning can occur within the 30-year time period, and this assumption must be kept in mind when interpreting the results of the study. This may not hold in cases of high-severity, stand-replacing forest fire. However, even when a

landscape is characterized as burned, it is likely to retain some unburned areas (e.g., Figure 4). Of note, any post-fire regeneration and associated fuel characteristics may be affected by climate, as well as by changes in fire frequency and severity.

1.2.2.2 Climate Data

Climate data were used to represent conditions and resources conducive to fire. At the 30-year resolution used for this study, these environmental characteristics include climatological normals rather than specific temporal patterns such as antecedent drought, or fire weather conditions such as a high wind day. In the development of the statistical models we ask, what are the long-term environmental characteristics that lead to landscapes having more or less fire? We selected variables representing spatial variability in the production of resources to burn, and in conditions that govern flammability and allow burning—such as seasonality. Five climate variables were selected from over 50 candidates describing moisture, energy, and water balance in the system. The selection of a handful of explanatory variables was necessary to avoid multi-colinearity in statistical models and allowed for parsimonious development of predictive models of fire frequency. Details of variable selection are found in Section 1.2.3 Statistical Modelling.

Data were provided for all watersheds draining into California at a spatial resolution of 270 m as 30-year averages for each month of the year. These data were generated from historical observations based on PRISM (Parameter-elevation Regressions on Independent Slopes Model) (Daly et al. 2004) data for 1971–2000, and from downscaled GCM projections for 2010–2039, 2040–2069, and 2070–2099. We clipped all data to the State of California and aggregated them to 1080 m landscapes to match the resolution of the fire data. All climate data were processed in the R programming environment.

Historical climate data used to generate 1971–2000 environments included temperature and precipitation data from the PRISM database, and additional variables associated with a regional water balance model called the Basin Characterization Model (BCM). Full details of the BCM are described in Flint and Flint (2007; 2012) and not included here. The BCM uses PRISM data downscaled by interpolation from native 4 km products to 270 m. Output products from the BCM include the water balance metrics described below, and a suite of others not used in our study (Flint and Flint 2012).

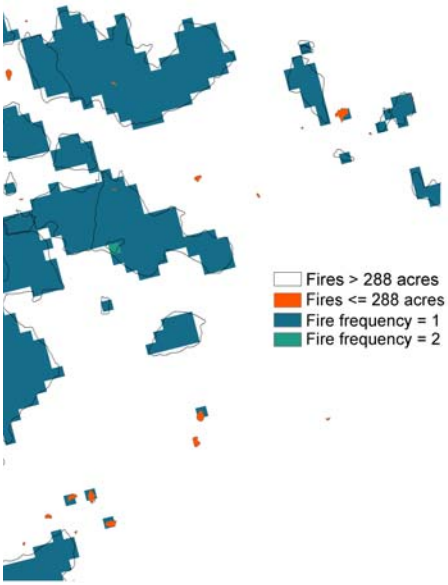

Figure 3: Processing Steps of Fire Polygons (Fires) to Fire Frequency Resulted in Simplification of the Raw FRAP Data, Including the Removal of Many Small Fires Due to Landscape Sampling Size and Processing Algorithms

Figure 4: The Mosaic of Unburned and Burned Patches of Chaparral Is Still Visible One Year After the 2007 Zaca Fire Outside of Santa Barbara, California. The sampling resolution of 1080 m simplifies these finer resolution patterns of burning. Fire burns with varying intensity resulting in heterogeneous severity within the perimeter recorded by the FRAP polygons. These patterns of severity are lost in our models of landscape burning, but are important to remember, since they contribute to post-fire structure and function of the ecosystem.

Photo Credit: Meg Krawchuk

The monthly climate data considered as potential contributing variables in the study included: maximum temperature, minimum temperature, total precipitation, potential evapotranspiration, climatic water deficit, and actual evapotranspiration. These variables are described briefly in Table 1; the reader can find detailed description of these variables in Flint and Flint (2012). Monthly normals were used to generate annual sum, mean, and standard deviation from these six metrics. Standard deviation was selected over a coefficient of variation as a measure of seasonality to avoid errors associated with zero-values in the denominator. Additional "Bioclim" variables were calculated from the monthly data but were all highly correlated with the six core climate metrics and their derivatives.

Future projections of climate variables for 2010–2039, 2040–2069, and 2070–2099 were generated from downscaled GCM output from NOAA's GFDL CM2.1 (National Oceanic and Atmospheric Administration's Geophysical Fluid Dynamics Laboratory model) and NCAR's PCM (National Center for Atmospheric Research Parallel Climate Model) under A2 and B1 emissions scenarios. The IPCC Special Report on Emission Scenarios (SRES; Nakicenovic [2000]) refers to A2 as a mid-high-emission scenario in which carbon dioxide (CO_2) concentrations reach 830 parts per million (ppm) by 2100. The B1 is a lower-emission scenario that can be viewed as a proxy for stabilizing atmospheric CO_2 concentrations at or above 550 ppm by 2100. As described in Cayan et al. (2008) and below, the GFDL has been used in California to represent a warmer-drier future, while the PCM represents a warmer-wetter future, though with only moderate increases in precipitation (Figures 5 and 6). The GCM data were downscaled to 12 km by researchers at Scripps Institution of Oceanography using the constructed analogue method (Hidalgo et al. 2008). These data were further downscaled by Flint and Flint (2007; 2012) to 4 km resolution for the purpose of bias-correction using historical PRISM data. The 4 km future projections were then downscaled to a 270 m using methods developed by Flint and Flint (2007; 2012), identical to those used to downscale the historical PRISM data. The 270 m data were used in the BCM to generate future projections of water balance metrics.

The GCM data used in this study were selected based three criteria, described more fully in Cayan et al (2008). Criteria included: (1) specific attributes of spatial and temporal resolution, (2) demonstrated skill in reproducing realistic historical climate characteristics for California, and (3) sensitivity to greenhouse gas forcing scenarios. Climate characteristics of particular interest for California included the distribution of monthly temperatures, seasonal cycle of precipitation, and spatial structure of precipitation (Cayan et al. 2008). The GFDL and PCM models provided the best fit to the stated criteria, based on comparisons to historical data completed by the PCM and GFDL groups, under the so-called 20C3M conditions. We refer the reader to Cayan et al (2008) for further details. Assessment of the two models by Cayan et al. (2008) show the increased annual temperature for both the GFDL and PCM correspond to greater increases in summer months of June, July, and August, in comparison to winter months of December, January, February. For example, in the period 2070–2099 under A2 emissions for northern California, annual temperature for the GFDL [PCM] is projected to increase by 4.5˚C [2.6˚C], with summer increases at 6.4˚C [3.3˚C] and winter increases at 3.4˚C [2.3˚C]. For precipitation, annual values for the GFDL [PCM] are projected to decrease 18 percent [2 percent], with summer decreases of 68 percent [30 percent] and winter

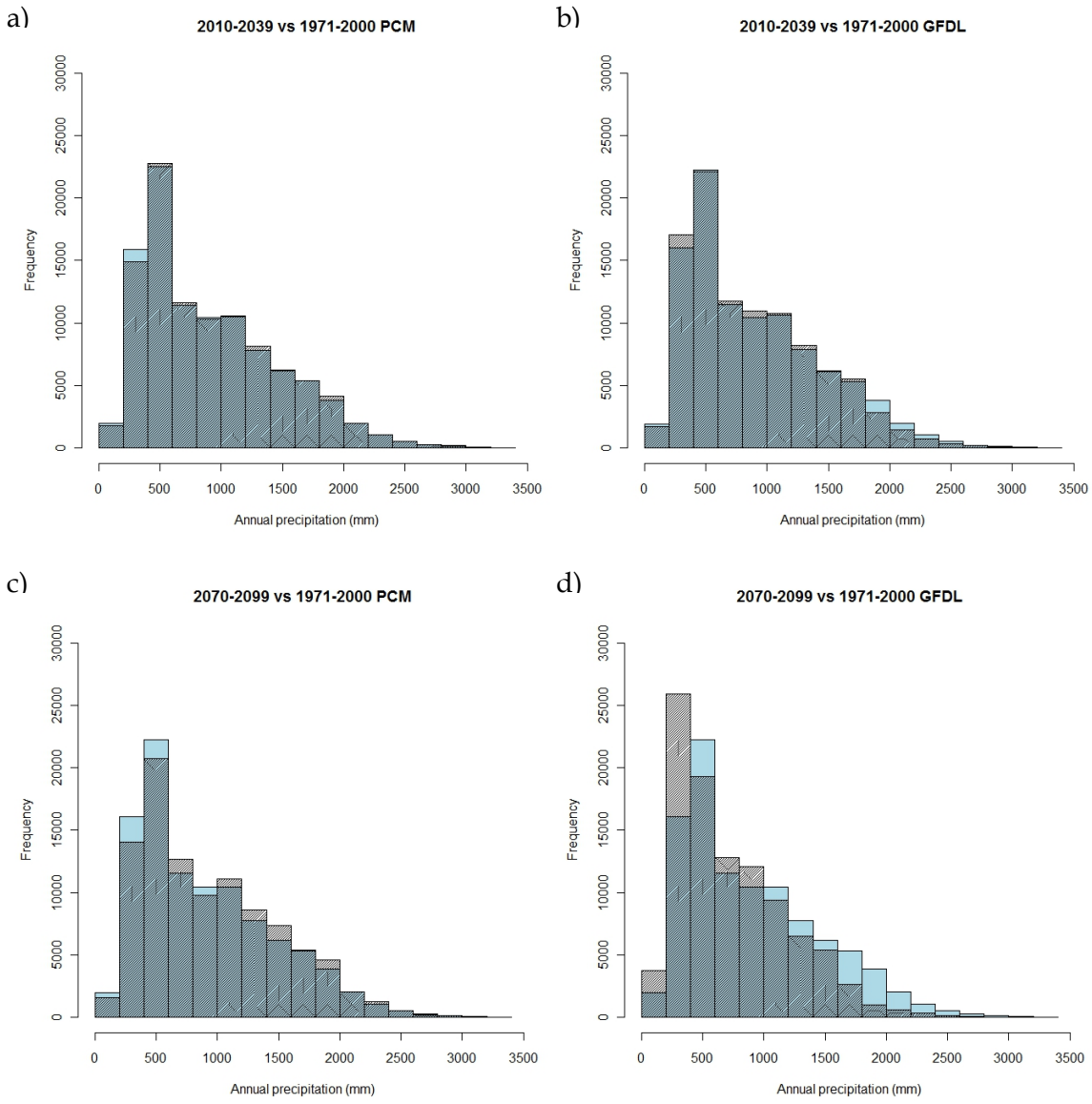

Figure 5: Changes in the Distribution of Annual Precipitation for 2010–2039 in the PCM (a) and GFDL (b) GCMs (Hatched) against Recent Historical 1971–2000 Conditions (Blue), and Changes for 2070–2099 for the PCM (c) and GFDL (d). Both GCMs project a warmer future for California, but the PCM projects warmer conditions with relatively modest increases in precipitation and the GFDL projects warmer-drier conditions. These differences are most obvious in the 2070–2099 data.

values decreasing 9 percent [increasing 4 percent]. For southern California, annual temperature for the GFDL [PCM] is projected to increase by 4.4˚C [2.5˚C], with summer increases at 5.3˚C [2.6˚C] and winter increases at 3.3˚C [2.4˚C]. For precipitation, annual values for the GFDL [PCM] are projected to decrease 26 percent [increase 8 percent], with summer decreases of 44 percent [11 percent] and winter values decreasing 2 percent [increasing 8 percent]. Overall, these seasonal breakdowns generally support the classification of the GFDL as warmer-drier relative to the PCM's warmer-wetter climate with respect to fire climate.

Figure 6 illustrates the placement of the PCM and GFDL models among an ensemble of 16 GCMs, based on annual precipitation and annual mean temperature for the entire study region. Values were calculated from global climate model output from the World Climate Research Programme's (WCRP) Coupled Model Intercomparison Project phase 3 (CMIP3) multi-model dataset (Meehl et al. 2007). Data were downscaled as described by Maurer et al. (2009) using the bias-correction/spatial downscaling method of Wood et al. (2004) to a 0.5 degree grid, based on the 1950–1999 gridded observations of Adam and Lettenmaier (2003). In the 2010–2039 period, the GFDL falls in the mid-range for temperature increases and low range for precipitation; the PCM falls in the low range for temperature and precipitation. By 2070–2099, the GFDL is still in the mid-range among GCMs for temperature but among the lowest of the 16 GCMs for precipitation. The PCM falls in the low range for temperature and low-mid range for precipitation; annual precipitation shows little change, but higher amounts than the GFDL. We refer to the PCM as warmer-wetter and GFDL as warmer-drier because of their contrast to one another; they do not represent bookends to the full 16 GCM ensemble. A complete ensemble analysis of future fire activity is beyond the scope of this study, but has been completed in other work, e.g., Moritz et al. (in review).

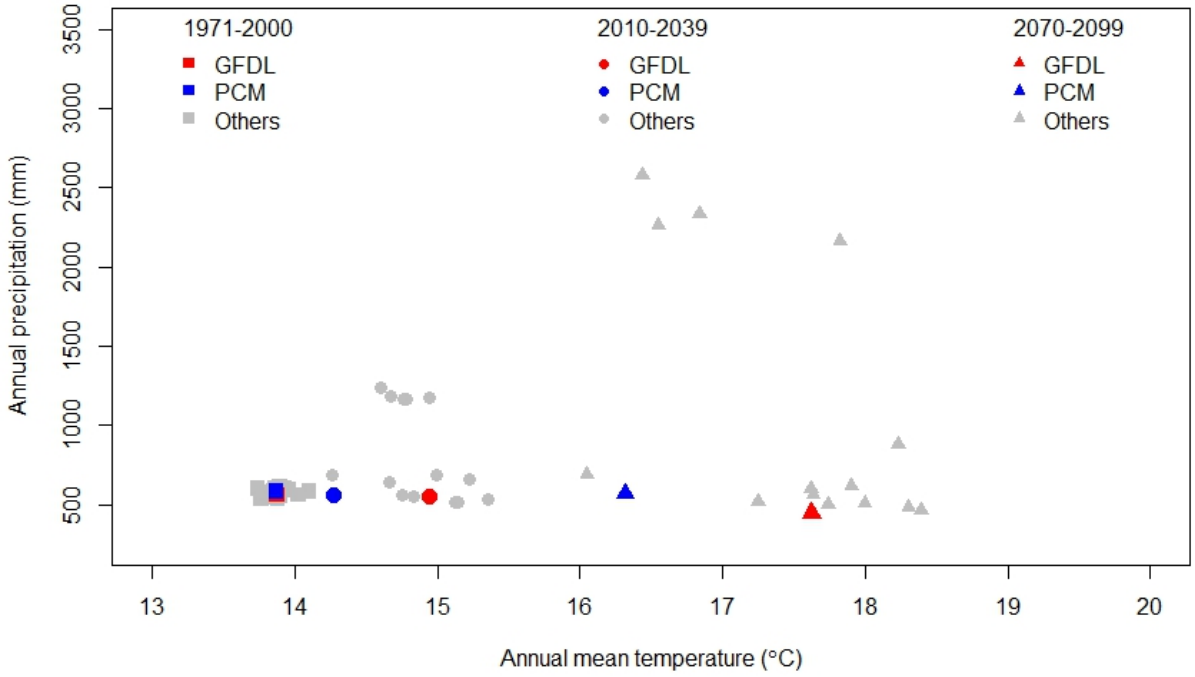

Figure 6: The Placement of GFDL and PCM GCMs within an Ensemble of 16 GCMs from the CMIP3 Archive. Note these are statewide annual mean temperatures and annual precipitation, masking much regional heterogeneity.

1.2.2.3 Data Quantifying Human Development

From fire records, we know that people cause many fires in California, but it is difficult to quantify complex mixtures of human behaviours into models of fire in a meaningful way. Fire management records suggest that roughly 85 percent of recent fires and more than 70 percent of areas burned in California were caused by people. Accordingly, this suggests that including patterns of human settlement and development in addition to climate might explain spatial

variability in California fire activity. Syphard et al. (2007) show that population density and distance to the wildland-urban interface contributed to explaining county-level patterns in fire frequency. The relationship with population appears to be hump-shaped, showing higher frequencies at intermediate levels; fire frequency decreases with distance to the interface. The distance to an urban interface incorporates the likelihood of someone starting a fire as well as the ease of access for fire-fighting operations, emphasizing the ambiguity in spatial metrics of human activity and outcomes on observed fire activity. Westerling et al. (2011) include a similar polynomial relationship between population and area burned on monthly resolved data for California, alongside climate relationships. Of course, these relationships from recent historical data are likely inadequate representations of eco-cultural fire relationships in the past, when firing of landscapes for hunting, agriculture, or aggression was likely more common (e.g., McKelvey et al. 1996). However, unless there are dramatic changes to policy and/or people's use of the environment, the coarse elements of recent historical relationships between fire and people are likely to persist through the twenty-first century.

The extent and type of current human development and potential future urban growth was characterized by data provided from the UPlan urban projection model. We used these data to develop two products, distance to development, and urban extent. Baseline data for UPlan characterizes urban, suburban, and exurban development in the year 2000 based on the National Land Cover Database (Vogelmann et al. 2001) and the California Augmented Multisource Landuse map (Hollander 2007). Potential future growth is generated as spatial projections of development for 2050 using demographic inputs and geographic data representing attraction and discouragement of growth. The UPlan characterization includes commercial and industrial development, and residential housing densities from 50 units/acre up to an exurban density characterized as 10-acre lots. Though these categories are available for future projections, the baseline data are a binary categorization of developed or not. A more complete discussion of this dilemma is provided in Bryant and Westerling's companion PIER paper. A spatial comparison of the baseline UPlan data and the Integrated Climate and Land-use Scenarios (ICLUS) 2000 (Theobald 2005), another common development dataset, showed that UPlan's baseline footprint is equivalent to the ICLUS 2000 categories one through six, characterizing densities up to and including 10-acre lots. Accordingly, the binary footprint of the baseline UPlan data represents the same categories that are included in the future projections simulated by UPlan. Fine-scaled rural development data are currently unavailable for California (Jim Thorne, pers. comm.), accordingly, rural development is not included in the UPlan model at this time; the minimum development density is a residential 10-acre lot. The ICLUS 2000 is based on census data and includes estimates of rural living to a metric of a > 160-acre lot; however, the coarse resolution of these data prevent direct incorporation into the UPlan framework.

Demographic data for the UPlan simulation model were taken from the Public Policy Institute of California, U.S. Census, Department of Finance, and InfoUSA. Development projections were run using two scenarios: a base and a smart-growth scenario. The base-case scenario used a business as usual (BAU) trend of development with no effort to restrict urban sprawl, including more of the population residing in lower-density residences. Smart growth uses rules to represent policy efforts to encourage growth in existing city centers, with more of the population residing in high-density living space. Details of the UPlan model and development scenarios can be found at http://ice.ucdavis.edu/doc/uplan. UPlan output was provided at a resolution of 50 m.

Distance to development (Figure 7) was used as a metric of isolation to test for a relationship between landscape fire frequency and human activity. Previous work has shown a strong effect of human development on fire in California, in particular, a negative relationship between distance to wildland-urban interface and human-caused fire (Syphard et al. 2007). This relationship highlights the increased likelihood of people starting fires closer to urban development. We developed metrics of linear distance to development from current development and projected growth from UPlan under the smart and business-as-usual scenarios (Figure 7). All categories of development were aggregated to the 1080 m landscape scale as binary classifications of developed or not developed, then Euclidean distance quantified the distance to development for every landscape in the study area. Distance to development does not fully cover human relationships with fire; further work into human activity metrics would be useful to pursue. No development data were available for island areas such as the Channel Islands, so distances were simply calculated as geographic distance to nearest mainland development. This treatment of islands is inadequate to characterize their true isolation, but was used as a general metric for this study. Many differences between the smart growth and business-as-usual scenario are obscured by the binary, landscape classification; however, key differences can be seen between the current and projected future patterns of development in Figure 7.

A measure of development extent was produced to be used as a mask indicating areas of infrastructure. This was used for mapping, but not in statistical analyses. Very low-density residential areas (10-acre lots) were omitted from the masks since these landscapes would be largely vegetated rather than urbanized. If these low-density areas were included, large parts of the state would be considered as developed, especially when aggregated to a 1080 m resolution. Using this criterion, 60,603 of landscapes are categorized as developed for the 1971–2000 time period. Under future projections for 2050 under smart growth, 65,711 landscapes are developed and under business-as-usual growth, 66,466 landscapes are developed. Many fine-scaled elements of growth are obscured by the 1080 m landscape classification, as was variability in the type of urban development such as industrial, commercial, and a range in density of residential land cover.

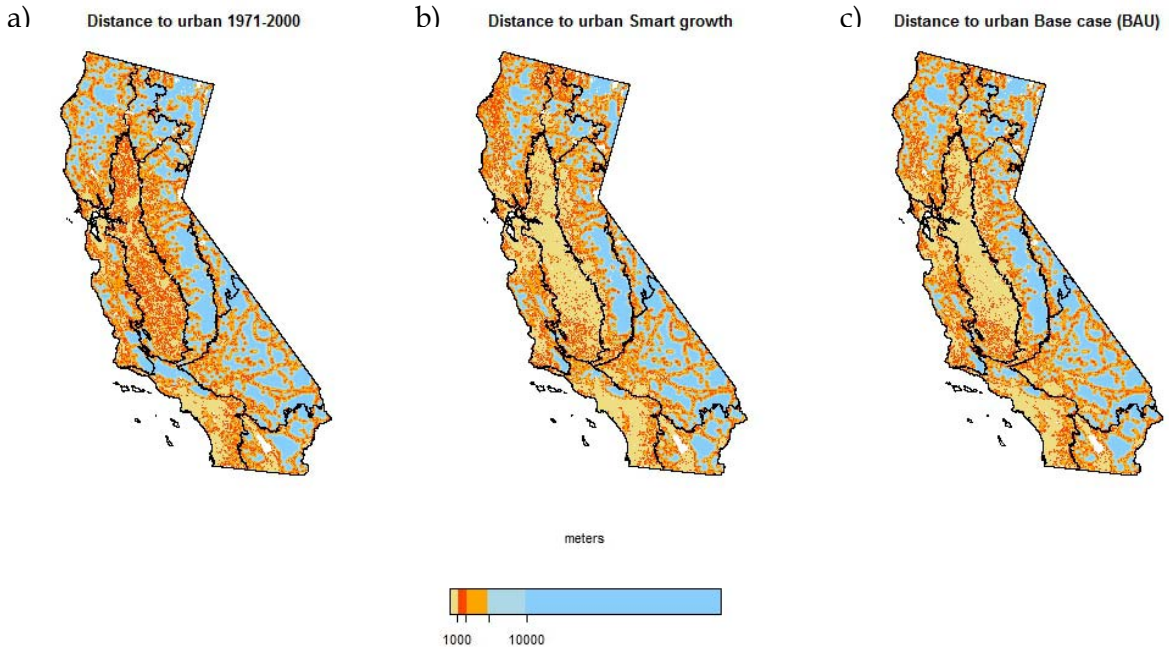

Figure 7: (a) Distance to Development Metric (D_dev) Generated from UPlan Data and Used for 1971–2000 Models, (b) Distance to Development Based on the UPlan Smart Growth Scenario, and (c) from the UPlan Base Case, Business-as-Usual Growth Scenario. Areas of water are shown in white, with the exception of islands that have been left blank, since our D_dev metric is somewhat arbitrary for them.

1.2.2.4 Land Cover Data

We used the multi-source land cover product from FRAP, fveg06_1 (http://frap.fire.ca.gov/) to identify water bodies and agricultural lands, and to use in our quantification of potential changes in fire frequency for key vegetation types based on California Wildlife Habitat Relationships (WHR). The original FRAP data were provided at a 30 m resolution, and we aggregated these to 1080 m based on the modal value of each landscape. We used the WHR 10-level coding to identify water and agricultural lands. These land cover types were masked from the dataset for statistical analyses since water is not likely to burn, and agricultural fires are not a direct focus of this study. The FRAP land cover dataset also includes an urban classification; however, we used the UPlan classification in our analyses. In general, the UPlan designation of development was equivalent to the FRAP land cover data, but in some cases more extensive, due to its inclusion of suburban and exurban residences.

We selected a group of WHR types for analysis of current fire frequency and potential future changes: Chamise-Redshank chaparral, Blue Oak woodland and Blue Oak-foothill pine (combined), mixed chaparral, Douglas Fir, Redwood, and Pinyon-Juniper. These types were selected to cover a range of different regions of California, and the authors' interest in these types.

1.2.3 Statistical Modelling

We developed statistical models of the relationship between fire counts and explanatory variables for the 30-year recent historical period from 1971–2000. The models used sparse sub-samples of the California-wide data and a zero-inflated Poisson structure. Ten iterations of the model were developed from random subsets of the recent historical data selected without replacement, following methods in Krawchuk et al. (2009). The parameters from each of these 10 models were then used with the full extent of explanatory data to produce a map of recent historical probability of fire, and the 10 models were averaged to produce a mean expected value for each landscape. For the projections of future fire, a similar approach was used, except simulated future climate and development data were incorporated with parameter estimates to predict the future distribution and frequency of fire. A variety of model methods can be used to examine relationships between fire and climate based on best judgment of researchers involved; here we provide outcomes of one such method.

Zero-inflated Poisson (ZIP) models accounted for the zero-heavy distribution of the count, or fire frequency data. Ignoring zero-inflation can result in biased estimation of parameters and standard errors (Zuur 2009). A binomial model of zeroes and ones might seem an attractive alternative, but the ZIP model structure allowed us to recognize that some landscapes burned more than once within a 30-year period (Figure 2). The ZIP model is a mixture of binomial and Poisson distributions, and allows for the inclusion of different explanatory variables in the binomial and count portions of the model. In the context of fire, zeros can arise for multiple reasons. We consider that the zero mass in the binomial component of the model could be generated from: unobserved or unrecorded fire, lack of an ignition agent regardless of suitable resources and conditions for fire, or misidentification of disturbance type (e.g., burned area documented as beetle kill). The explicit consideration for absence of an ignition agent in flammable locations is a key element of this model structure. In the Poisson, or count, component of the model we consider zeros to be a function of un-suitable "habitat" for fire such as excessively moist conditions or an absence of resources to burn as found in deserts, barrens, or mountain rock. These areas are contrasted against those where fire does occur, one or more times within the sampling interval. For the ZIP model it is unnecessary to split data into the binomial and Poisson components of the mixture *a priori*, rather, model estimates are generated from statistical hypothesis we prescribe based on our pyrogeographic theory.

1.2.3.1 Model Development and Assessment

Model development required five steps: identification of sub-sample size, selection of explanatory variables from candidate pool, development of model structure, model fitting, and the validation and assessment of final models.

The identification of a meaningful sub-sample size was necessary because patterns of burning and environmental covariates are all spatially structured. A benefit of this sparse sampling approach was it leads to development of general fire frequency models, rather than modeling the specific spatial patterns of fire observed in the training period of 1971–2000. We used a conservative approach to identify a sampling fraction that would result in both an absence of autocorrelation in model residuals and a meaningful effective sample size for statistical hypothesis testing. The approach we used was to identify a sampling fraction of the landscape fire data that would result in spatially random point patterns of fire occurrence, based on a Ripley's K-function using a convex hull border to frame the analysis. We masked the landscape fire data to remove water, wetlands, agriculture, and urban areas. Given the large proportion of

ones, we used areas burned as a binary classification, ignoring the number of times burned for the analysis. From this analysis we selected a sampling fraction of 2 percent, corresponding to 5254 samples used for development of each of the 10 models.

Selection of variables to include in the statistical models required the identification of metrics from a suite of over 50 candidates, many of which were correlated to one another. Although multicollinearity does not affect the use of statistical models to infer the mean response under observed conditions, it can make interpretation of variables difficult because parameter estimates are conditional on other variables in the model, and valid predictions can only be made if multicollinearity patterns hold for the new data. Given the goal to use these models predictively for future climate no-analogue structure, this latter point is particularly important.

We used a two-step approach, first screening variables to identify a handful that would characterize unique information, then defining our pyrogeographic hypotheses to be represented by these variables in the model structure. We used pairs plots and Pearson correlations to reduce the candidate pool, and for those remaining fit binomial generalized additive models (gams) to determine which of two "tied" variables explained more variation in landscape burning. Nine variables remained after this screening. We then fit binomial gams to 10 iterations of 2 percent subsets of these data to identify strong relationships and suggest appropriate response forms, such as second-order polynomials. The final set of variables from this selection procedure are described in Table 1 and Figure 8, and include maximum monthly temperature, precipitation seasonality, potential evapotranspiration seasonality, actual evapotranspiration seasonality, and climatic water deficit. Quadratic forms of the terms for seasonality in actual evapotranspiration and in maximum monthly temperature were found to improve the fit of data. The term for distance to development rarely contributed to explaining variability in landscape burning, even with a quadratic term, but we opted to include the term so that some element of human influence would be maintained. It is likely the weakness in this relationship occurred because we include both human- and lightning-caused fire together in our analyses.

From the finalized candidate pool, we identified variables that characterize resources for burning, conditions conducive to fire, and ignition. At a 30-year climatological scale, information about dry, warm periods and seasonality included: maximum temperature, precipitation seasonality, and potential evapotranspiration seasonality. Spatial variability in a warm, dry season that converts potential fuels to available fuels (Pausas and Keeley 2009) provides information about conditions conducive for burning. Information on variability in resources available for burning through growth form, productivity, and community composition included: climatic water deficit and actual evapotranspiration seasonality.

Table 1: Explanatory Variables Used in Statistical Models. All climate variables were quantified as a 30-year climatology for 1971 to 2000.

Variable	Acronym	Description	Range min-max [median]	Source
Maximum temperature	TMax_ave	30-year mean of the maximum monthly temperature (°C). A measure of energy in the system.	3–33°C [21°C]	Scripps/ PRISM, BCM input
Precipitation seasonality	Ppt_seas	Standard deviation for the year, of 30-year mean monthly precipitation (mm). A measure of moisture in the system.	2–225 mm [35 mm]	Scripps/ PRISM, BCM input
Potential evapotranspiration seasonality	PET_seas	Standard deviation for the year, of 30-year mean monthly amount of water that can evaporate based on radiation, shading, vegetation. A measure of energy in the system	35–69 mm [57 mm]	BCM input
Actual evapotranspiration seasonality	AET_seas	Standard deviation of the year, of 30-year mean monthly water evaporated (mm). PET when soil water content is above wilting point. An integration of energy and moisture in the system.	0.009–70 mm [25 mm]	PRISM, BCM output
Climatic water deficit	CWD_sum	Annual sum of annual water deficit, from 30-year mean monthly values (mm). The difference between PET and AET, quantifying when evaporative demand exceeds available water. An integration of energy and moisture in the system.	0–1543 mm [861 mm]	PRISM, BCM output
Distance to development	D_dev	Distance to areas designated as developed in the UPlan framework, in meters.	0–40,000 m [3,830 m]	UPlan

PRISM are model input data (Daly et al. 2004), BCM is the Basin Characterization Model (Flint and Flint 2007; 2012)

Previous work has shown that water deficit and evapotranspiration describe variation in vegetation very well (Stephenson 1998). Here we used a seasonality term (AET_seas); however, the spatial pattern of variability in the annual sum of AET was very similar to AET_seas. Though we present these variables in categories of resources and conditions, they likely share information describing these elements. Distance to development was included as a proxy of likelihood of human ignition. One could also consider the probability of burning to be a function of whether a neighbouring cell burns and previous fire activity in the landscape, but at a coarser temporal perspective used here we suggest these are subsumed by conditions generated through environmental characteristics.

Each of the 10 ZIP models was fit using the six terms and two quadratic forms (Table 2). We identified the best model structure based on these eight terms with the Akaike Information Criterion (AIC), using three sub-sample sets for model testing. Model selection through AIC can be strongly affected by spatial structure in data (Hoeting et al. 2006), and accordingly, the sparse sub-sampling approach used here contributed to robust model selection. In the binomial component of the final model structure, we included: AET_seas and its quadratic, PET_seas, Ppt_seas, and D_urb. In the Poisson component of the model, we included: CWD_sum, TMax_ave and its quadratic.

Parameter estimates from each of these models were used with the full data set from 1971–2000 to generate estimates of the probability of landscape burning zero, once, twice, three times, and so on, and the expected number of fires, for a 30-year interval. The estimated values from each of the 10 models were averaged for each location to produce a surface quantifying the mean probability of burning at least once, and two or more times in a 30-year interval. We calculated a mean fire return interval for each landscape (mFRI) using 30 ÷ n, where *n* is the mean expected number of fires for each landscape over the 30-year period.

Statistical significance, contribution to the model, and variation explained by variables was assessed using p-values of Chi-square tests and AIC. Model fit was assessed using plots of Pearson residuals against fitted values and explanatory variables, and of fitted values against observed data. We also examined differences between fitted and expected count probabilities, as suggested by Lambert (1992). These tests were done against the training data themselves, as well as against the 98 percent of data withheld from the subset model. A final test of temporal transferability was completed by developing models using fire, climate, and urban infrastructure data from the 30-year period from 1941–1970 using the same methods as for 1971–2000, and comparing the probability of fire from those models to those predicted from the 1971–2000 model parameters but incorporating climate and development data from 1941–1970. Results of the temporal transferability validation are presented in Section 2.

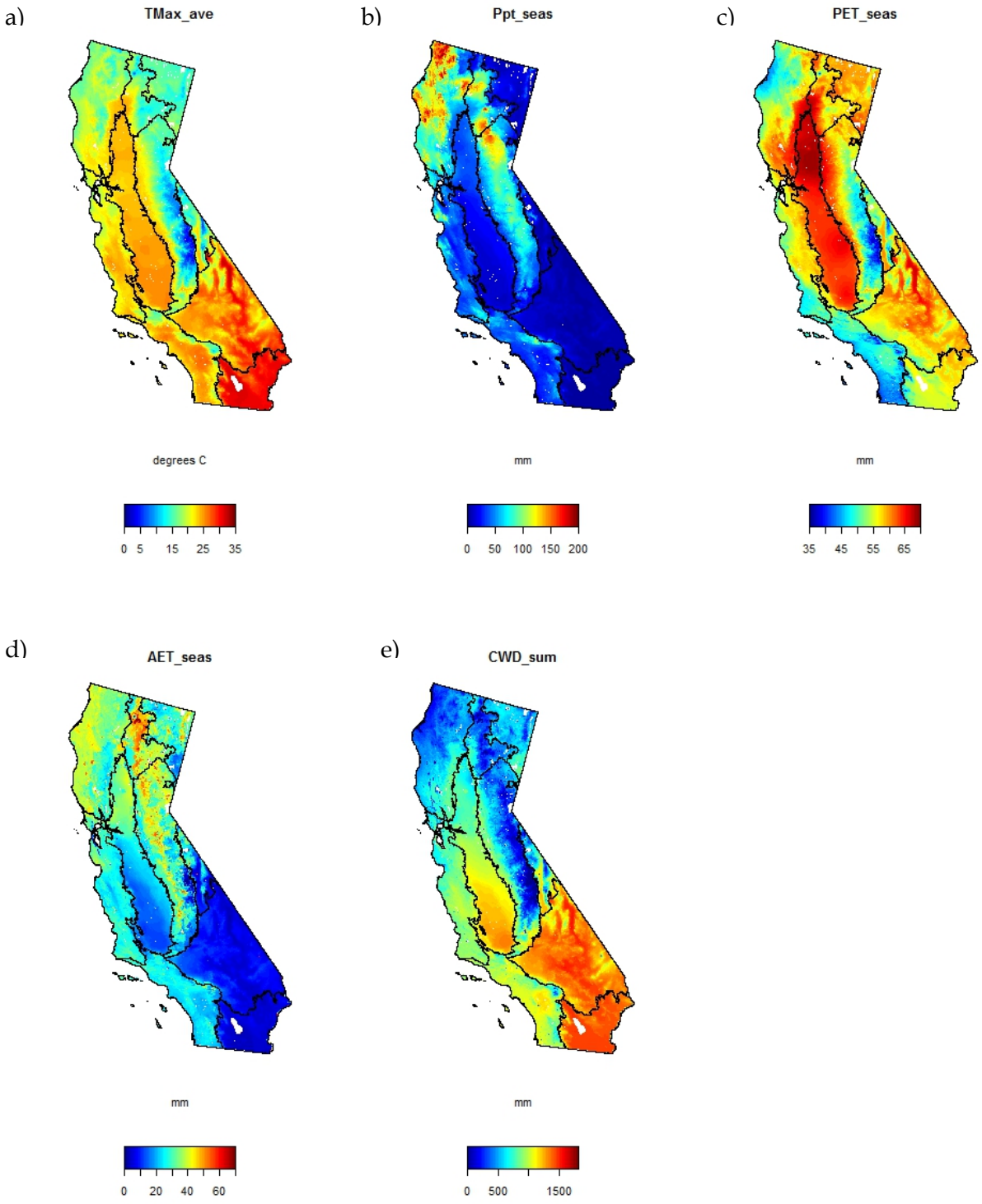

Figure 8: Spatial Patterns in Explanatory Climate Variables for 1971–2000. (a) Maximum monthly temperature, (b) seasonality in precipitation, (c) seasonality in potential evapotranspiration, (d) seasonality in actual evapotranspiration, and (e) annual climatic water deficit.

1.2.3.2 Model Projections

The 10 models of recent historical landscape burning were built using random samples of the 1971–2000 fire, climate, and urban infrastructure data. Parameters from these models were used with future climate and urban development projections to predict future probability of landscape fire. Projections were generated for situations characterizing 2010–2039, 2040–2069, and 2070–2099 using the GFDL and PCM GCMs under the A2 and B1 emissions scenarios. For each of these situations, we projected fire probabilities using the base case and smart growth UPlan urban projections. Though these UPlan projections were generated for 2050, we used them for all future situations. For the near-term (2010–2039) situations, we also predicted fire probability with no change in development infrastructure. In total, projections included three time periods, two GCMs, two emissions scenarios, and two urban growth projections. For simplicity, here we report on near future (2010–2039) and distant future (2070–2099) situations from both GCMs, using the A2 emissions scenario and the UPlan Base case urban growth projections.

A technique called *clamping* is frequently used in complex modeling frameworks such as Maxent. Clamping means that values falling beyond the range of the explanatory variables used in model fitting are set to either the minimum or maximum value. The goal is to avoid uncertainty in results that occur due to the extremely non-linear and convoluted shapes of response curves that can be fit by these types of models. We used very simple response forms in our models, either linear or quadratic; accordingly, we did not clamp our future projections. We assumed that the simple forms used in the statistical models would make them robust to predictions of future climate.

We examined the stability of models built from the mean of 10 random samples of data by running model estimates on 50 random samples, then calculating the probability of burning at least once under 1971–2000 conditions and 2010–2039 conditions using the GFDL A2 climate data and Base case UPlan data. We then calculated the change in probability of burning for the 10- and 50-replicate averages to determine if the estimates were stable.

1.3 Results

1.3.1 Model Assessment and Validation

Each of the variables included in the statistical models varied slightly in their explanatory power of variability in landscape fire among the 10 sub-models used to develop the mean probability of fire. Table 2 summarizes the overall ranking in explanatory power of each variable (Table 2: AIC Ranking) using a metric of the ranked order based on the magnitude of change in AIC when each term was dropped from the model. AET_seas and its quadratic contributed most strongly to the models, followed by PET_seas. The urban metric, D_dev contributed least to the models. The polarity of parameter estimates (Table 2: Relationship) was consistent among models. An illustration of the shape and turning points for TMax_ave and AET_seas main effects and their quadratics are shown in Figure 9.

Plots of model residuals against fitted values and fitted versus observed showed no discernible pattern, however the count portion of the model appeared less well fit than the binomial one. The metric outlined by Lambert (1992) based on the difference between predicted probability of each count value and the observed probability is shown in Figure 10, where values above zero indicate that a model overestimates the probability, and below zero indicates underestimation.

The metric illustrates relatively little difference between predicted and observed probabilities but where differences occur, the general pattern is for an overestimate of zero and two, and an underestimate of the value of one. Figure 11 illustrates patterns from tests against the data used to build the models, similar patterns were found when tested against the 98 percent of data withheld from model development.

Table 2: Model Assessment and Validation

Variable	AIC Ranking	Relationship	Component of the model
AET_seas	1	+	Poisson
AET_seas^2	2	-	Poisson
PET_seas	3	-	Poisson
Ppt_seas	4	+	Binomial
CWD_sum	5	+	Binomial
TMax_ave	6	+	Binomial
TMax_ave^2	7	-	Binomial
D_dev	8	+ (ns)	Binomial

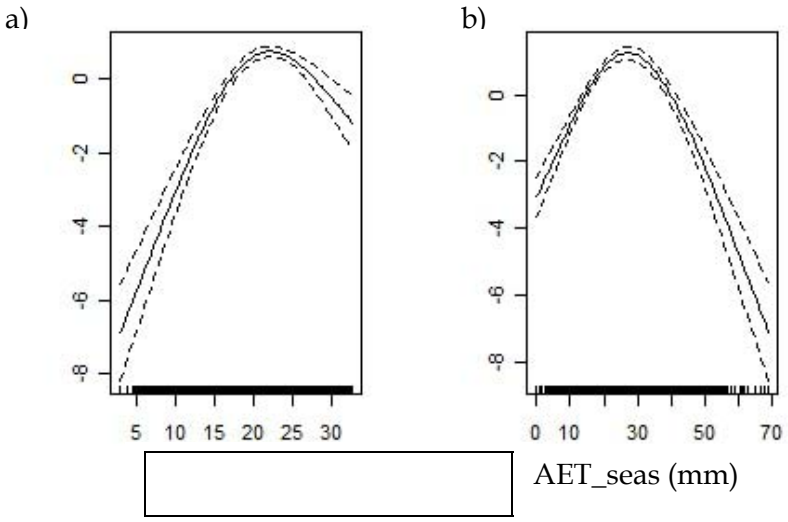

Figure 9: Exemplar Shapes of Quadratic Relationships for (a) Maximum Monthly Temperature, and (b) Seasonality in Actual Evapotranspiration, from One of the Ten Models

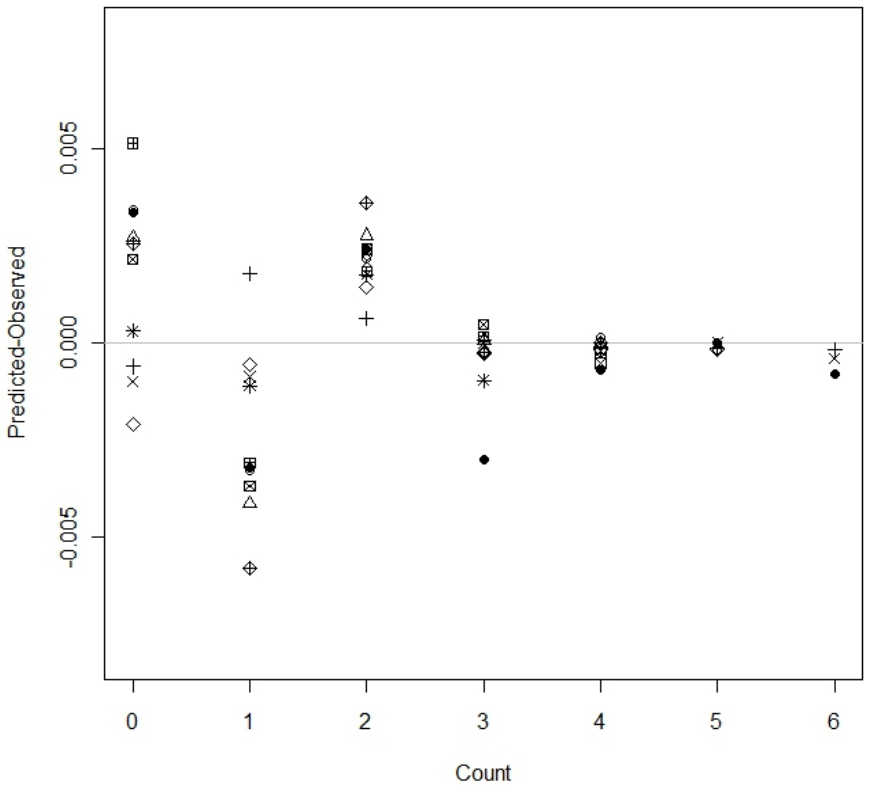

Figure 10: Assessment of Zero-inflated Poisson Models Using the Difference between the Probabilities of Predicted and Observed Counts for Each of the Ten Sub-models

1.3.2 Current and Future Fire

Estimates of current landscape fire and projections of future fire were generated for each of the 10 models, then averaged to produce a single surface for each time period. Based on the modeling strategy and temporal resolution used in this study, projected changes in future fire need to be interpreted carefully. Remember, models included environmental variables describing both resources and conditions for burning, and accordingly, changes in fire are a result of shifts in resources or conditions, or both elements together. While conditions for fire vary simultaneously with climate, it is unlikely that vegetation resources will have the ability to shift in pace with climate change, especially in the near term. Projections for 2010–2039 should be interpreted as climate space in transition, where fire weather conditions are likely to track climate change quite closely, yet resources to burn may lag behind in. By 2070–2099, vegetation resources are more likely to have shifted in response to changing climate; however, even then, it is questionable what resources will be available given proposed no-analogue conditions, mixtures in community assembly, and the outcomes of transitions periods.

Illustrations were generated for the probability of at least one fire and for the probability of two or more fires. Delta maps were generated to highlight areas of change, where the difference between current and future fire probability was calculated for each of the 10 models, then averaged. Predictions were generated for the entire area of California, but for illustrations we masked areas of urban infrastructure, water, and agriculture for a clearer focus on areas of

interest. Jepson ecoregions were superimposed on all figures to aid in georeference. Figure 11 shows the progression of the probability of at least one fire in 1971–2000, the delta, and the probability in 2010–2039 under Base case urban projections for the GFDL and PCM under the A2 emissions scenario. Figure 12 is a similar illustration, but highlights the probability of two or more fires in a 30-year period. As can be noted from the change in scaling on the legend, two or more events within a 30-year period are much less likely than a single event, but still relatively common in the southwest of California. The 2070–2099 time periods are illustrated in Figures 13 and 14, and illustrate more dramatic changes in the frequency of fire associated with climate changes projected through the end of the twenty-first century. Variation in polarity of change predicted by the GFDL and PCM for 2010–2039 and 2070–2099 are illustrated in Figure 15 by showing areas where models agree on increases in fire, agree on decreases in fire, and areas where they disagree.

1.3.3 Mean Fire Return Intervals, mFRI

The mFRI is useful for understanding the fire environment, and considering potential ecological consequences of predicted changes in fire produced by changes in climate and urban growth. The mFRI provides a more intuitive metric than the probability of fire by estimating the time between fires. Figures 16 and 17 illustrate the mFRI for 1971–2000 versus 2010–2039 and 1971–2000 versus 2070–2099 for the GFDL and PCM GCMs. The boxplots shown in Figure 18 illustrate the spatial distribution of mFRI values for key WHR vegetation types under current and future conditions.

In comparing the values reported here to observed fire frequencies, it is important to recognize that these values represent the mean of an expected frequency. Random deviates generated from these expected values would more closely represent observed events. For the calculation of mFRI, we used $30 \div n$, where n is the mean expected event count estimated from our models. If as a representative example we generate a single iteration of 10,000 random deviates from the zero-inflated Poisson (count) distribution with mean expected event count of $n = 0.4$ and probability of zero = 0.8, we find an outcome of 4 events predicted during a 30-year period occurs 3 times, 3 events occurs 14 times, 2 events occur 105 times, 1 event occurs 494 times, and zero events occur 9384 times. Transforming these values into mFRI metrics, we would have return intervals ranging from 7.5 years (for 4 events/30 years) representative of landscapes burning multiple times within the 30-year study interval, to zero (0 events/30 years) for landscapes never burning in the study interval. These specific outcomes are all possible, with varying probabilities, under the same generating function or mean expected value.

1.4 Discussion

Climate changes projected for California in the next century imply dramatic alteration of fire frequency from what we have experienced in the recent past. While our study includes projections from just two GCMs, these models have been selected for their skill in reproducing historical climate for the region, and bracket warmer-drier and relatively warmer-wetter (little change in precipitation) simulations of future climate. In general, the statistical fire model predictions show a greater change in the probability of burning in the distant future (2070–2099) than near future (2010–2039), as would be expected from the greater changes in climate by the end of the century. The magnitude of changes in the probability of burning were much greater for those landscapes likely to incur increases (i.e., more fire) than decreases, with most extreme increases roughly three to four times greater than extreme decreases. In general, the direction of

projected change was the same for the probability of at least one fire, and for two or more fires, but there were exceptions, largely in drier landscapes in eastern California. This variability in projected changes between more fire-prone landscapes and less fire-prone ones emphasizes differences in the controlling factors that deserve further attention in future work. Our quantitative framework does not explicitly model vegetation and changes therein resulting from altered climate; however, this information is implicitly accounted for in our macro-scaled modeling approach using explanatory variables representing resources, conditions, and ignitions required for fire.

The statistical models used here have shortcomings in representing transient dynamics of climate change. The time period 2010–2039 should, in general, be interpreted as fire-climate space in transition, where fire weather conditions are likely to track climate change quite closely, yet resources to burn may lag behind. However, the approach used here assumes vegetation/resources to burn track climate in real time; this is not necessarily a valid assumption, especially in situations with rapid climate change within a short time period. Our model projections for 2070-2099, when vegetation resources are more likely to have shifted in response to changing climate may match rates of change in climate, vegetation, and fire more appropriately; however, even then, it is questionable what resources will be available given proposed no-analogue conditions, mixtures in plant community assembly, and the outcomes of transitions periods. In previous work, we have held vegetation constant in near term projections and let fire conditions change (Krawchuk et al. 2009). Each method has benefits and caveats. Landscape and/or regional simulations with fire and vegetation sensitive to climate variability are a tool with great potential for integrating this type of relationship in future work.

By 2070–2099, the spatial extent of increases and decreases in probability of landscapes burning at least once varied dramatically between the PCM and GFDL GCMs, especially in the desert areas of southeastern California, the Modoc Plateau, and around the periphery of the Great Central Valley. The warmer-drier conditions simulated by the GFDL GCM projected decreased fire in these already xeric areas; whereas, the warmer-wetter PCM projected increases. This type of response has strong support from existing research on varying constraints of fire in resource-rich and resource-poor environments (Krawchuk and Moritz 2011; Littell et al. 2009; Westerling and Bryant 2008; van der Werf et al. 2008; Gedalof et al. 2005; Westerling et al. 2003; Swetnam and Betancourt 1990), where more precipitation in hot and dry, resource-poor landscapes has been shown to increase fire through the production of vegetation to burn, as was the case during the 2011 fire season in Arizona and Texas. In contrast, continued drying and warming in these areas likely leads to decreases in vegetation amount and connectivity through physiological stress in these challenging environments. In the remaining, more resource-rich areas of California, there was general agreement between GCMs for an increased probability of one or more fires per 30-year period in the future.

Previous work on future climate change and fire in the western United States has largely focused on area burned, whether at an annual or monthly scale. Projected patterns of area burned for ecoprovinces in the western U.S. with a 1°C (1.8°F) increase in global average temperature and a suite of GCMs (National Research Council 2011), based on Littell et al.'s (2009) methods show general similarity to our results from the warmer-drier GFDL projections with large increases in fire for Northwestern California, Cascade Ranges, and the Sierra Nevada; decreased area burned is projected for the Mojave and Sonoran Deserts. Outcomes disagree for the Modoc Plateau region and areas around the Great Central Valley, suggesting

further inquiry could be useful in these areas. Large parts of Southwestern and Central Western California were not included in the Research Council study, and these are the regions where our models projected some of the most dramatic increases in the probability of fire by 2070–2099, for projections of at least one fire and for more than two fires.

A second source of comparison is Westerling et al. (2011) future projections of monthly area burned for California, which also shows the same ilk of spatial patterns as our projections, and similar spatial disagreement on increased and decreased fire between GFDL and PCM GCM outcomes. Our projections were developed at a much finer spatial resolution, but coarser temporal resolution than Littell's or Westerling's work, and it is encouraging to note the similarities among the studies. We suggest the finer spatial resolution provided by our work could be helpful in local, topoclimatic scales aimed at examining texture in future patterns of burning, which is critically important for understanding ecological effects of changes in fire and landscape management.

Studies of the probability of fire at similarly fine-scaled resolution to our work have been completed for California in the past, but focus only on the relative probability of recent historical fire (Parisien and Moritz 2009, Waller et al. 2007, Parisien et al. 2012). Here, we have refined methods to be based on more simplistic model forms, developed methods for counts of burn events rather than presence/availability used in these previous studies, and used climate projections to make predictions of the risk to changes in future fire. The probability of burning multiple times within a 30-year interval was modeled through the Poisson mixture of the ZIP statistical model and allowed used to identify landscapes with the potential for burning more than once, twice, or more over three decades. In Section 2, we also examine the application of our methods to previous climates by back-casting the probability of fire to 1911–1940 and 1941–1970 periods. This retrospective analysis provides good support for our forward projections, but also highlights specific areas where back-casts do not align with observed data, providing food for thought in subsequent work.

The back-casts to the 1941–1970 time period are informative as a proof-of-concept for our methods, since we have fire records from that period. Though fires were not as rigorously documented in this earlier time period, it is useful to examine the back-cast projections against estimates generated from that period as a form of validation. In addition to differences in recording of events, human behavior both in suppression and in fire use is likely to have changed in the past, so appropriate caveats must be included. Even though the metric of distance to development did not rank highly in our models, there is no question that people contribute to burning patterns in California given that fire management records indicate roughly 85 percent of recent fires and more than 70 percent of area burned in California was caused by people. For our future projections, we assume that the general fire-climate-human behaviours, including ignition, suppression, and fire and land management will follow similar patterns to what have occurred in the period 1970–2000; this may or may not be true. For example, if drastic changes in fire policy or of human land use were to occur, projections could have much less relevance.

Islands are interesting things, from the perspective of biogeography, cultural diversity, and pyrogeography. The Channel Islands off the coast of Southwestern California were included in our analyses; however, we have concerns about the validity of estimates produced for them. Due to the modeling approach, the island climates are considered equally to those on the mainland; however, estimates might be off due to differences in fire activity attributable to

smaller and more isolated areas. For example, they are less connected, and these smaller landscapes tend not to burn as frequently as similar mainland ones, since fire spread from neighbouring lands is much reduced. Though not explicitly islands, continued land cover change and fragmentation could render many mainland landscapes as fire "islands" and also alter their likelihood of burning. These landscape effects were not included in our models; this "island pyrogeography" deserves further development in future work.

We were surprised that a metric of distance to development showed no relationship to fire counts, given it is well known that humans are responsible for starting a large number of fires in California. Over the period of 1971–2000, the FRAP fire database lists 877 fires caused by lightning, only 15 percent of the total number, yet 23 percent of the area burned over the period. While the attribution of cause of fire may not be correct all the time, the general pattern highlights that humans cause a lot of burning.

Our inability to detect an effect may likely be explained by fire spread. One might expect human factors to affect the number of fire ignitions, but unless these occur under conducive fire weather conditions they will not grow to be large enough for detection and recording. Because of the very weak, negative relationship between the probability of burning and distance to development, our projections for smart growth and base, business-as-usual, urban growth were very similar. Accordingly, we only present results from the projections of fire under business-as-usual future growth. In future work, it would be interesting to develop more sophisticated metrics of development and population. For example, work by Westerling et al. (2011) focused more specifically on wildland-urban interface in statistical models of both lightning and human caused fires, using population, and vegetation fraction per cell as metrics of human effect on area burned. Bryant and Westerling's work in this iteration of the PIER project addresses these ideas more specifically.

The mean fire return interval metric, mFRI, allows us to consider the fire frequency that biota may have been exposed to over the recent historical record, and how this might change in the future. For example, an increase in the recurrence of fire could threaten some California ecosystems (Keeley 2005) and remove species from a vegetation community, even if they do already experience fire quite frequently. Species could be filtered out if they experience insufficient time to reach maturity, and/or if seed banks have been exhausted in previous fires, or inadequate resources have been stored for re-sprouters to survive. Accordingly, even fire-prone environments could be at risk to fire-induced ecosystem change due to increases in frequency. In contrast, reduced fire frequency could pose challenges for fire stimulated species, or those requiring post-fire environments for establishment. It is also important to keep in mind that alteration in the return interval of fire is just one way in which climate change might alter fire regimes. Fire severity, seasonality, size, and frequency all contribute as components of the ecological process of fire.

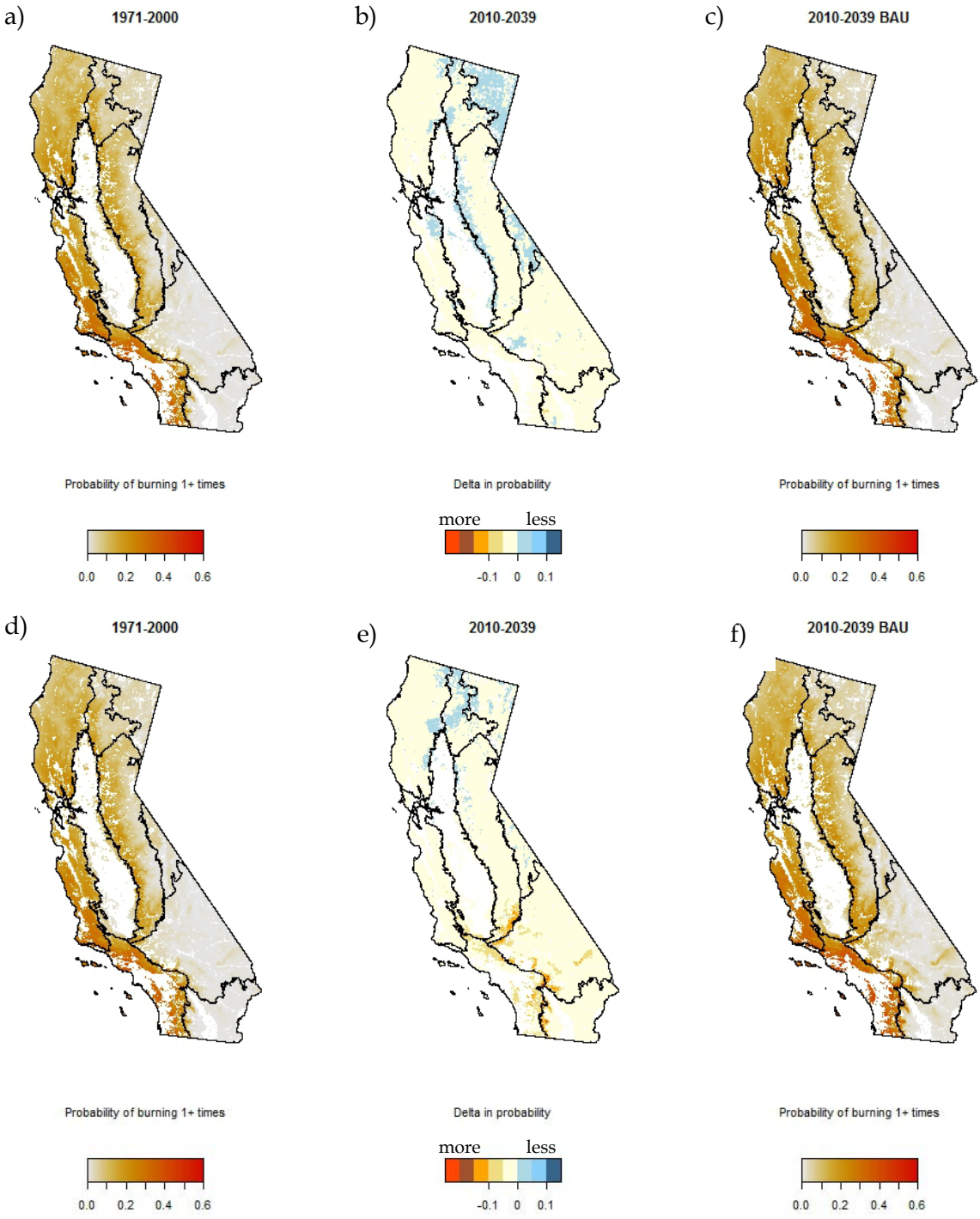

Figure 11: (a) Probability of Burning at Least Once under 1971–2000 Conditions, (b) Change in Probability by 2010–2039, and (c) Projected Future Probability over Thirty Years for 2010–2039 Based on the "Warmer-Drier" GFDL GCM, A2 Emission Scenario and UPlan Base Case Urban Growth. (c–d) projections Using the "Warmer-Wetter" PCM GCM. Areas of water, agriculture, and urban infrastructure are masked in white, with the exception of low-density residential housing (see Methods).

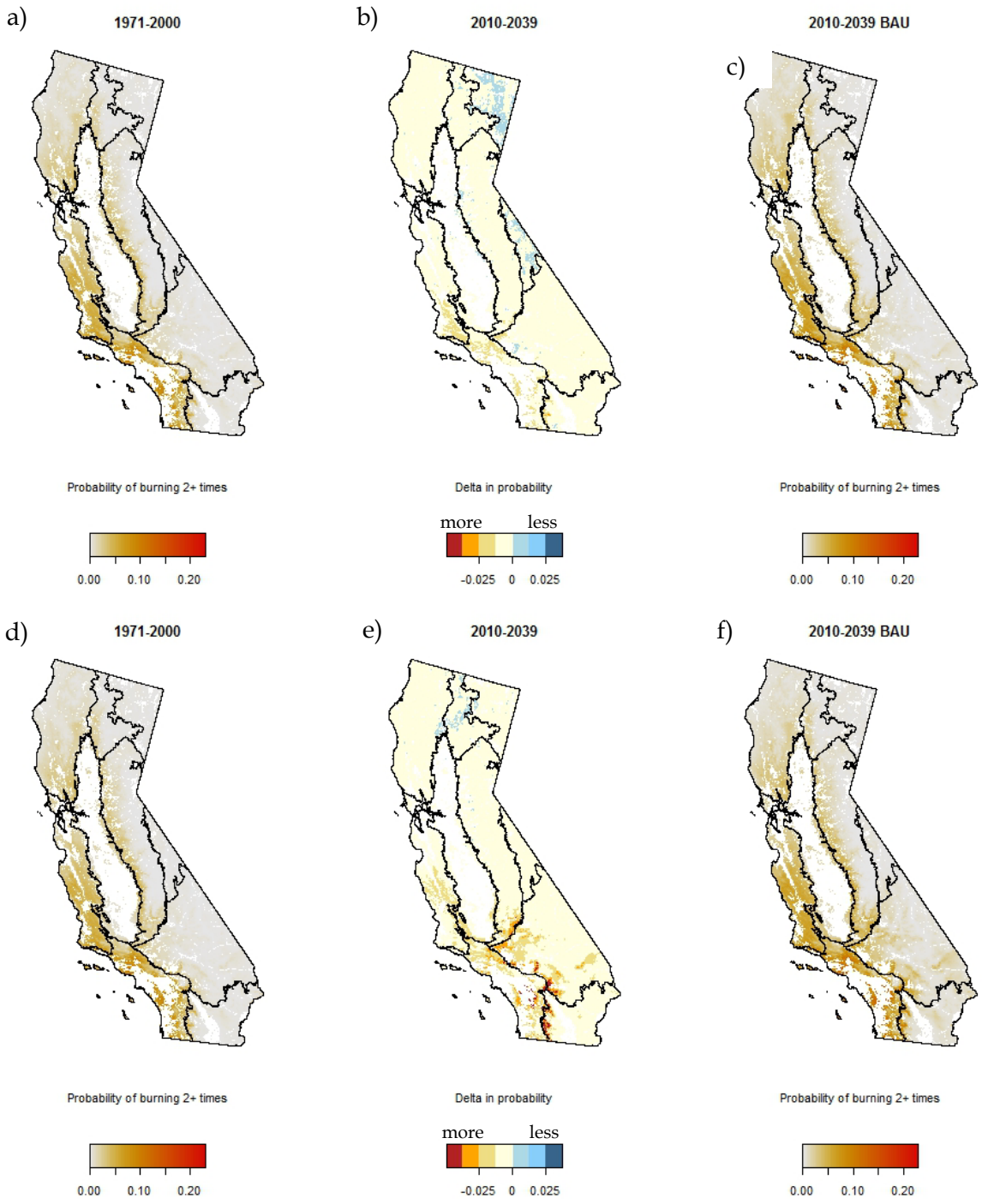

Figure 12: (a) Probability of Burning Two or More Times under 1971–2000 Conditions, (b) Change in Probability by 2010–2039, and (c) Projected Future Probability of Burning Two or More Times for 2010–2039 Based on the GFDL GCM, A2 Emission Scenario and UPlan Base Case Urban Growth, and (d–f) Projections Using the PCM GCM. Areas of water, agriculture, and urban infrastructure are masked in white, with the exception of low-density residential housing (see Methods).

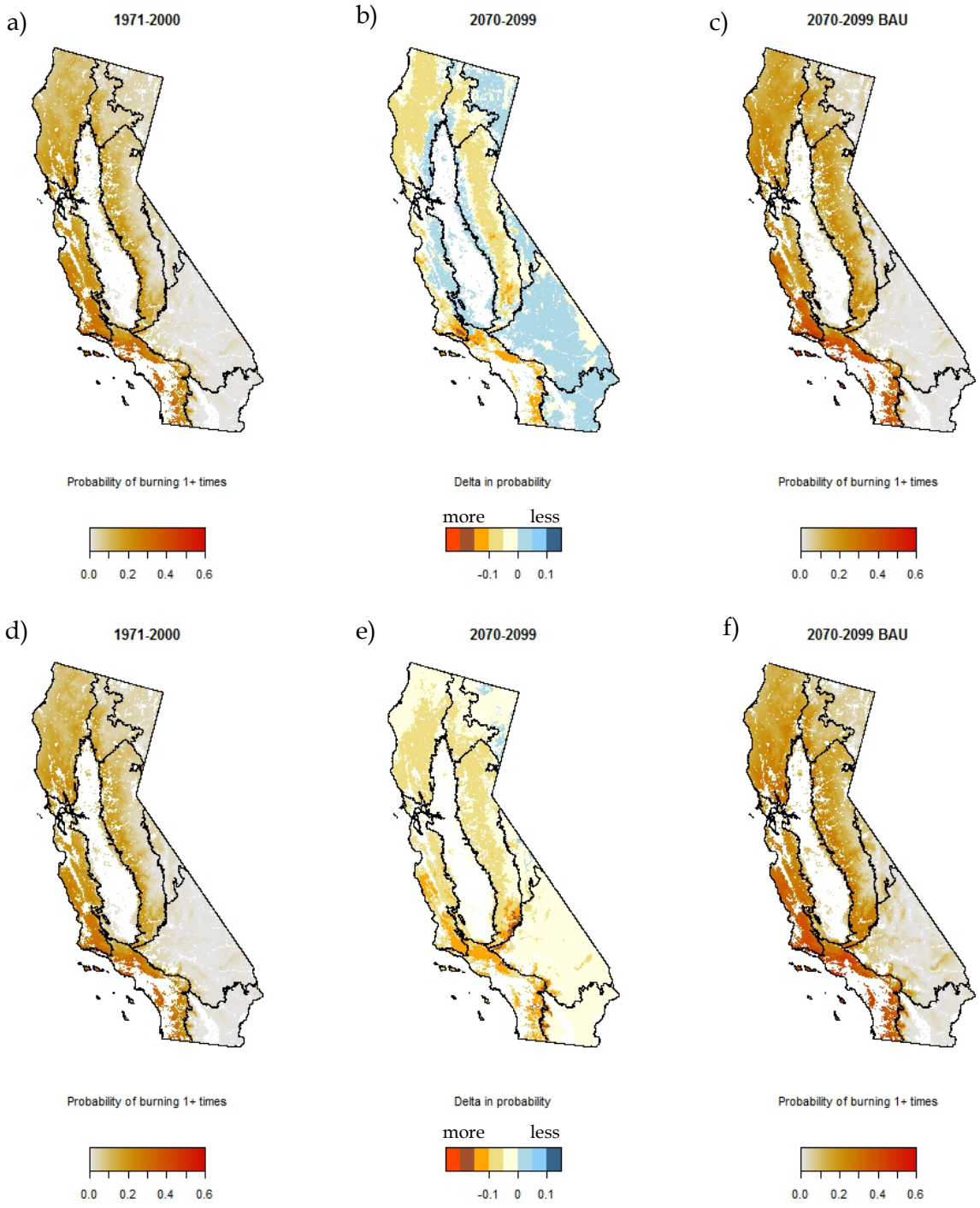

Figure 13: (a) Probability of Burning at Least Once under 1971–2000 Conditions, (b) Change in Probability by 2070–2099, and (c) Projected Future Probability of Burning at Least Once over Thirty Years for 2070–2099 Based on the GFDL GCM, A2 Emission Scenario and UPlan Base Case Urban Growth. (d–f) projections using the PCM GCM. Areas of water, agriculture, and urban infrastructure are masked in white, with the exception of low-density residential housing (see Methods).

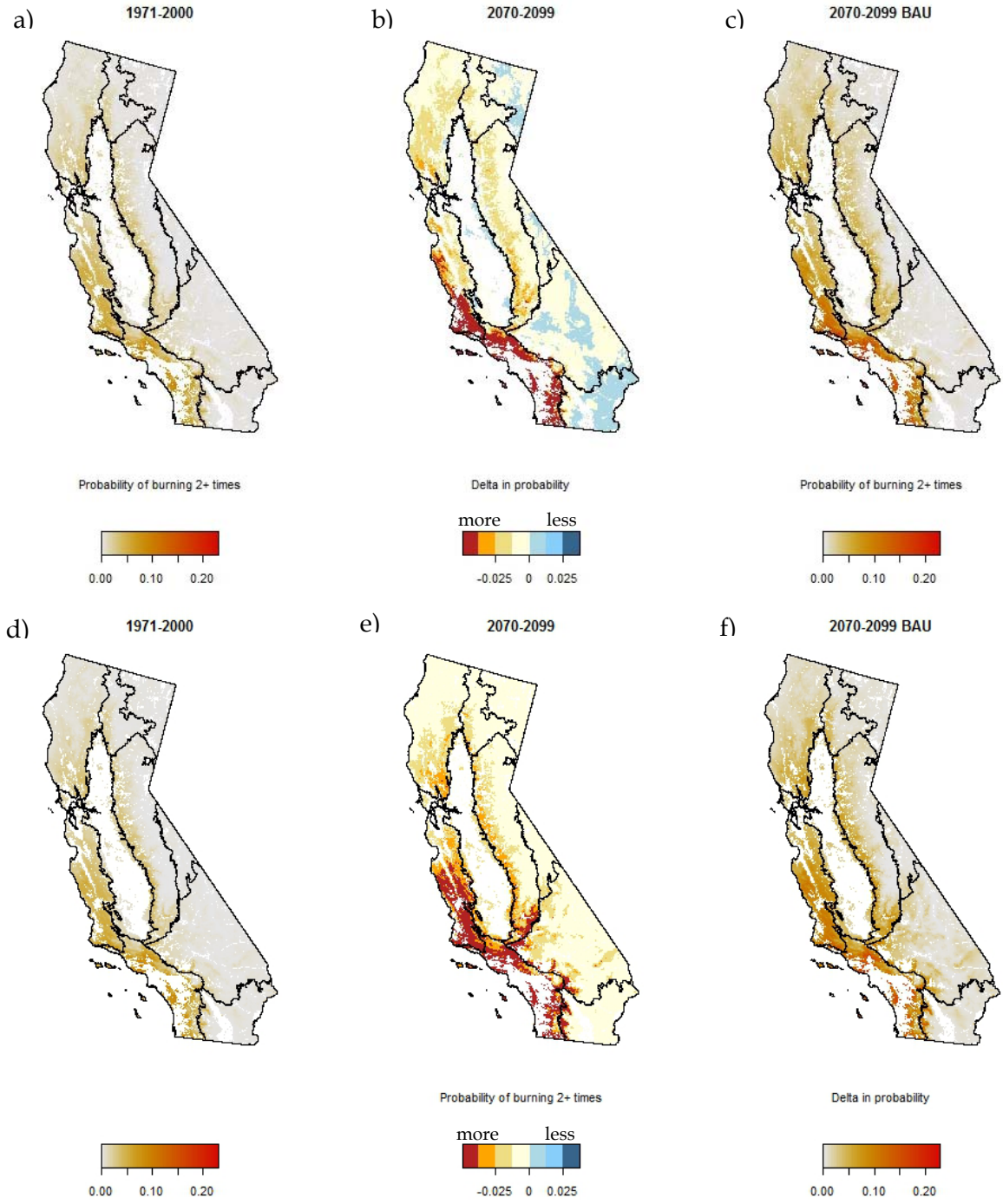

Figure 14: (a) Probability of Burning Two or More Times under 1971–2000 Conditions, (b) Change in Probability by 2070–2099, and (c) Projected Future Probability of Burning Two or More Times for 2070–2099 Based on the GFDL GCM, A2 Emission Scenario and UPlan Base Case Urban Growth. (d–f) projections using the PCM GCM. Areas of water, agriculture, and urban infrastructure are masked in white, with the exception of low-density residential housing (see Methods).

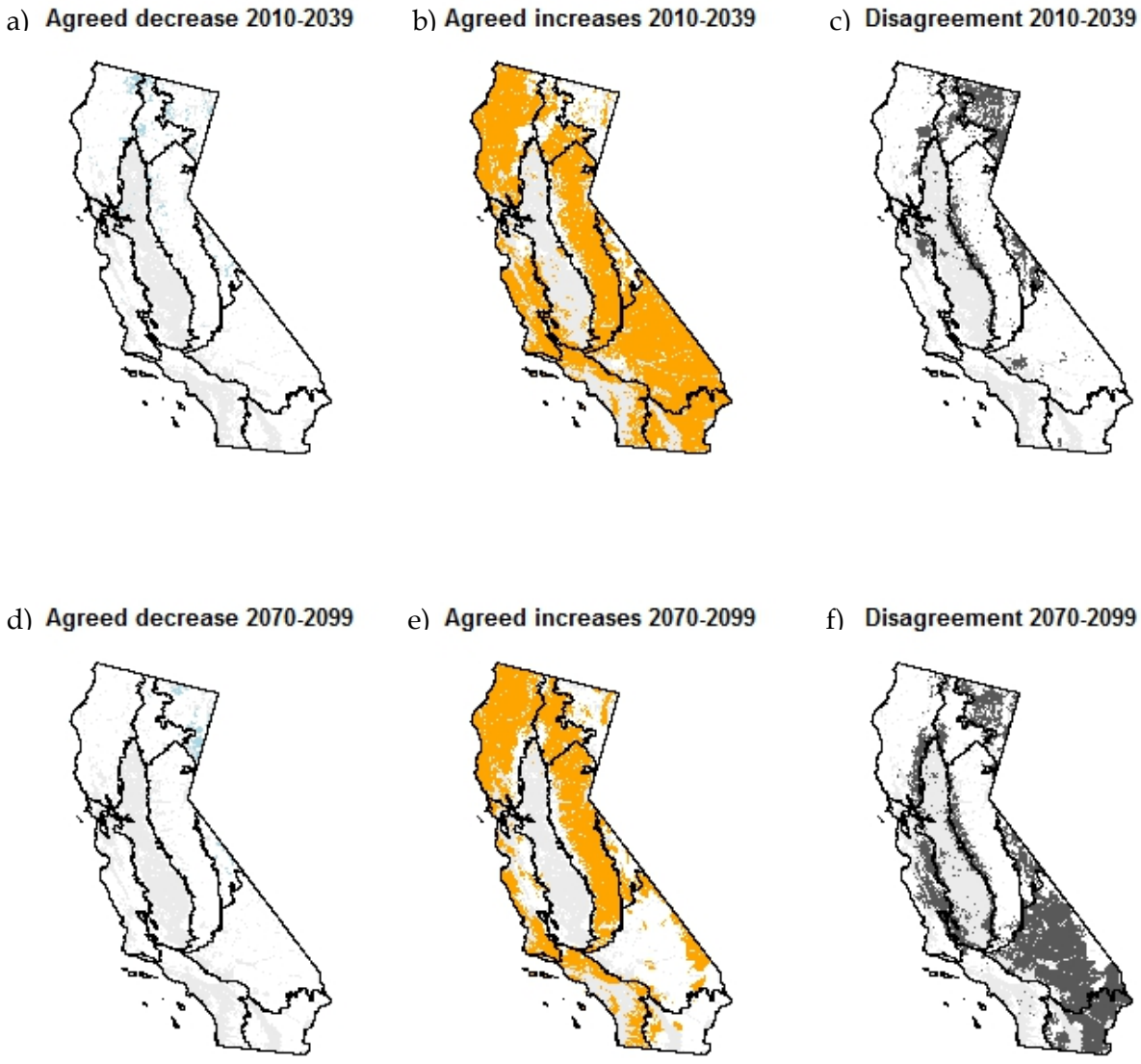

Figure 15: Agreement in Decreased and Increased Projected Changes in at Least One Fire (a,b) and Disagreement (c) for 2010–2039, and 2070–2099 (d–f). Areas of water, agriculture, and urban infrastructure are masked in light grey, with the exception of low-density residential housing (see Methods).

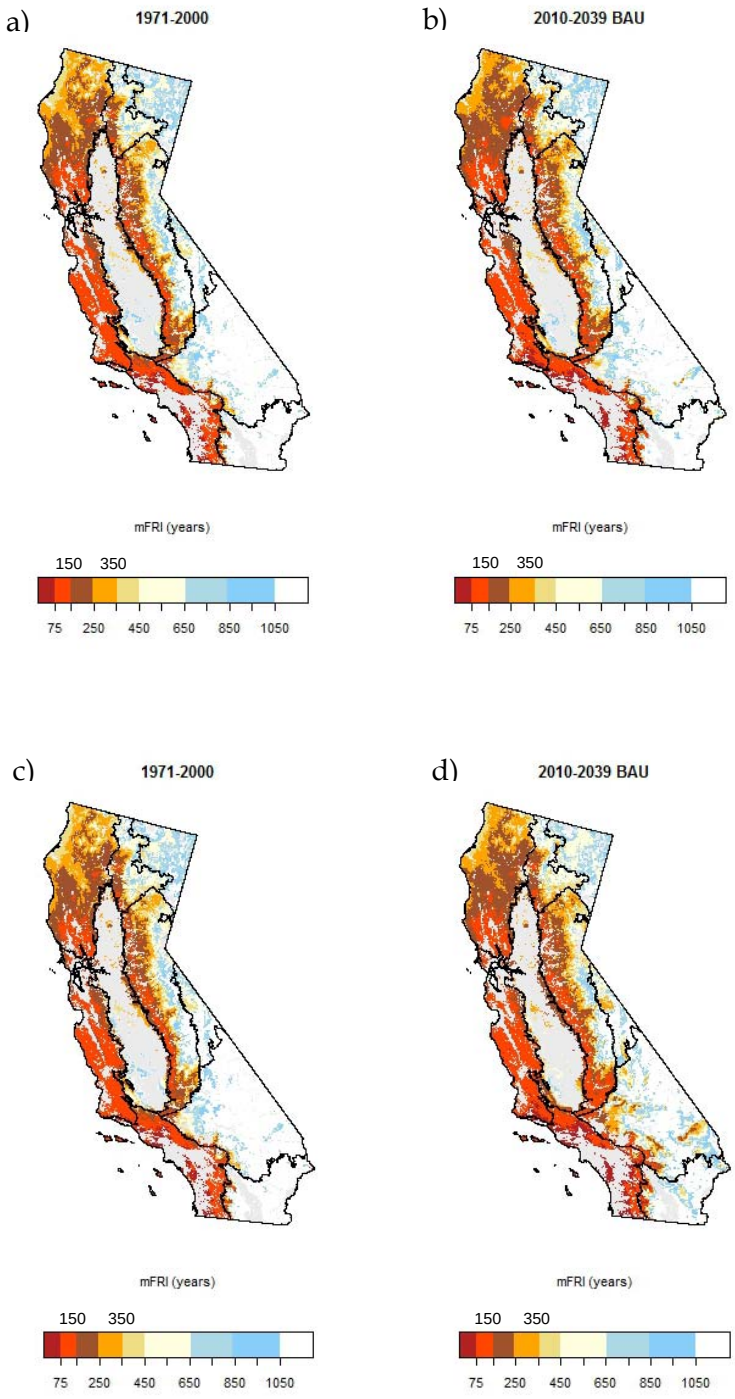

Figure 16: Mean Fire Return Interval (mFRI, 30 ÷ Expected Number of Fires) for 1971–2000 and 2010–2039 for (a,b) GFDL and (c,d) PCM GCMs. Urban, agricultural, and water are masked in grey.

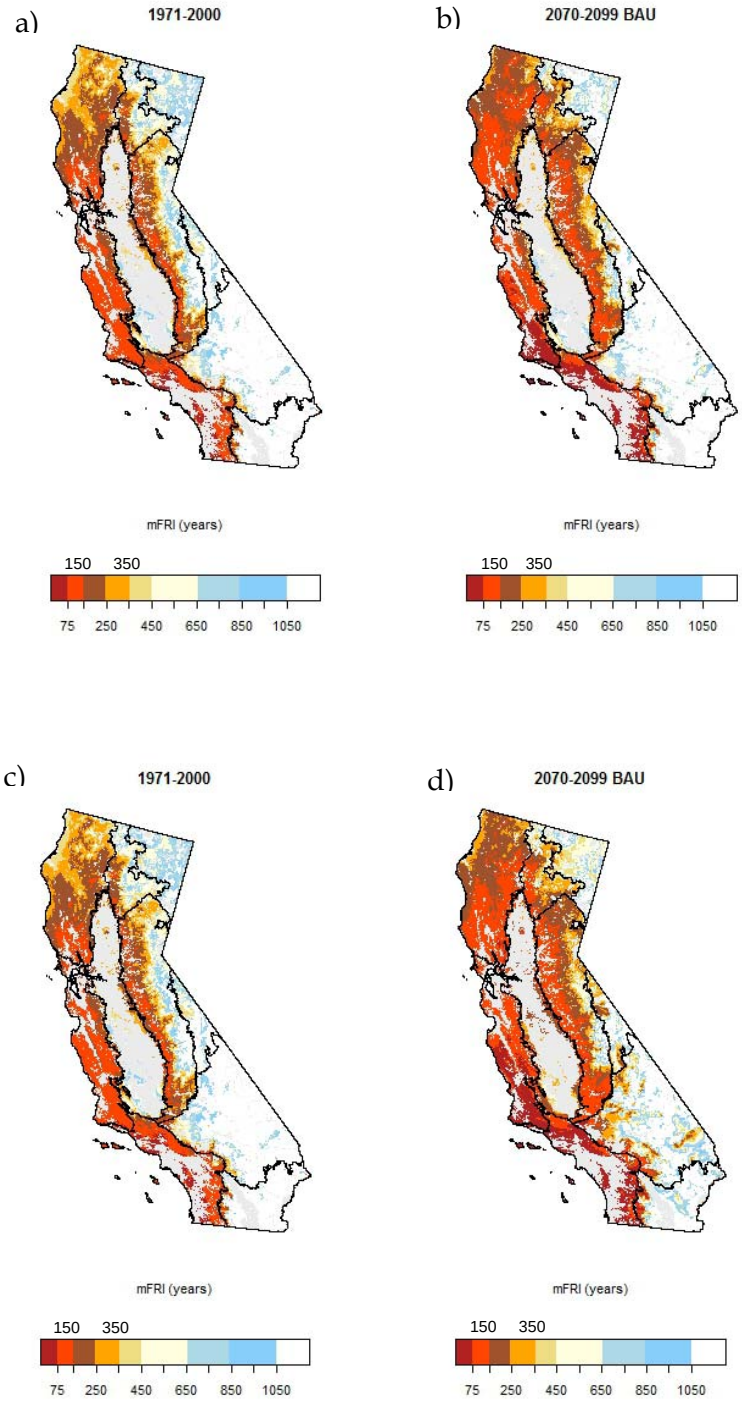

Figure 17: Mean Fire Return Interval (mFRI, 30 ÷ Expected Number of Fires) for 1971–2000 and 2070–2099 for (a,b) GFDL and (c,d) PCM GCMs. Urban, agricultural, and water are masked in grey.

a)

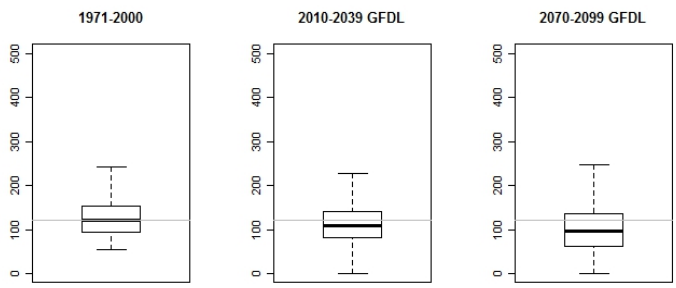
1971-2000
2010-2039 GFDL
2070-2099 GFDL
0
100
200
300
400
500

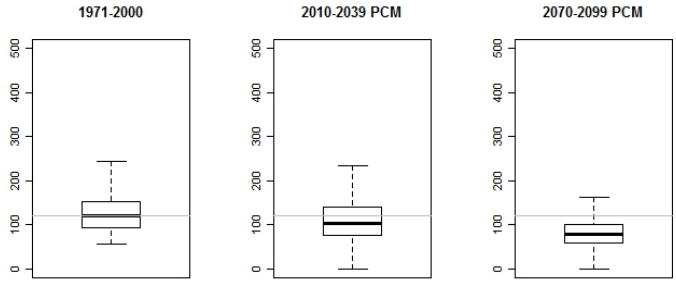
1971-2000
2010-2039 PCM
2070-2099 PCM
0
100
200
300
400
500

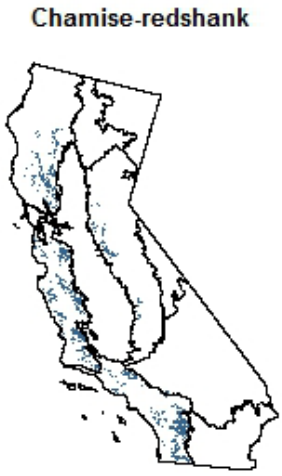
Chamise-redshank

b)

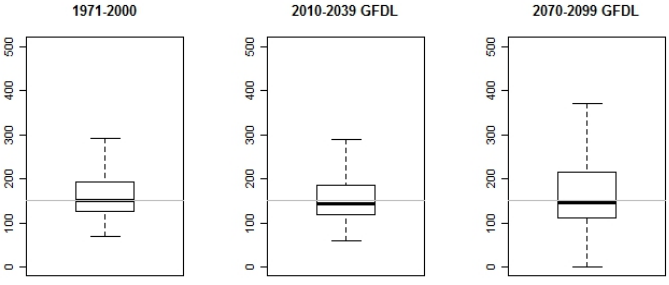
1971-2000
2010-2039 GFDL
2070-2099 GFDL
0
100
200
300
400
500

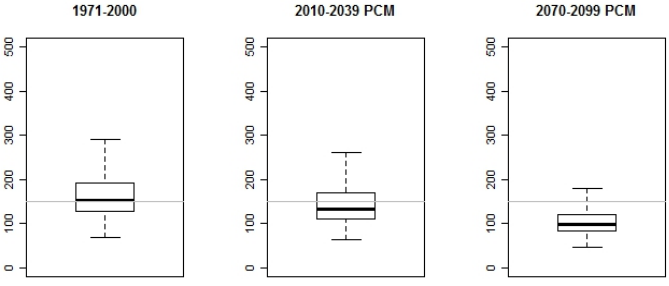
1971-2000
2010-2039 PCM
2070-2099 PCM
0
100
200
300
400
500

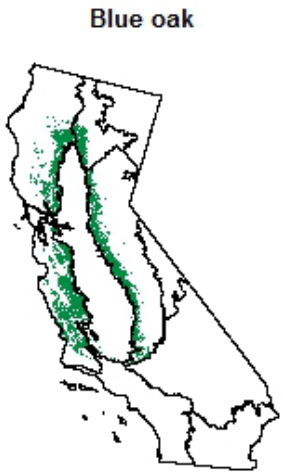
Blue oak

c)

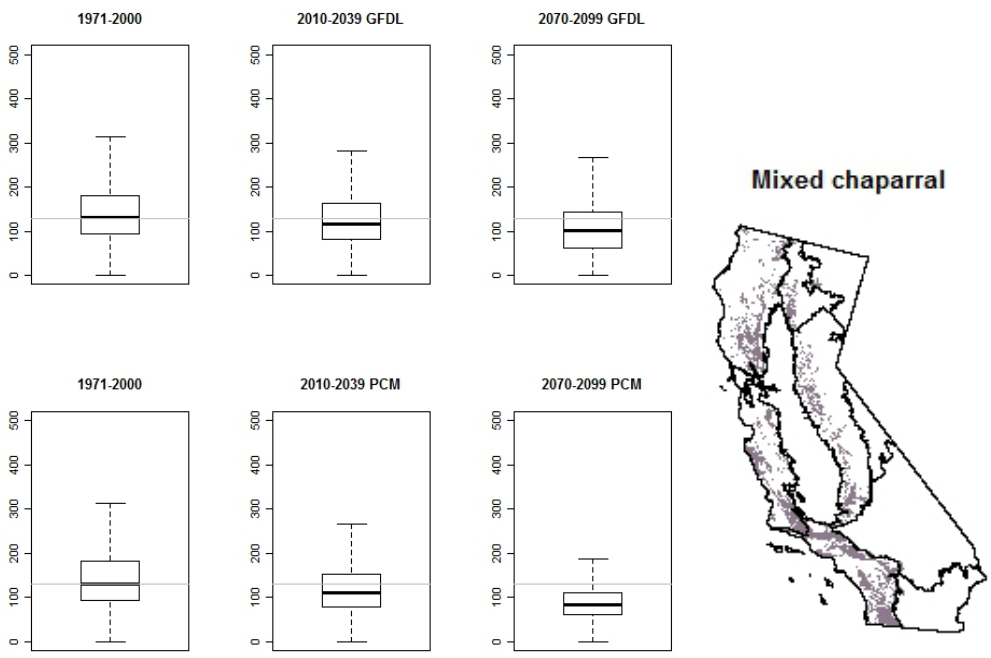
1971-2000
2010-2039 GFDL
2070-2099 GFDL
1971-2000
2010-2039 PCM
2070-2099 PCM
Mixed chaparral

d)

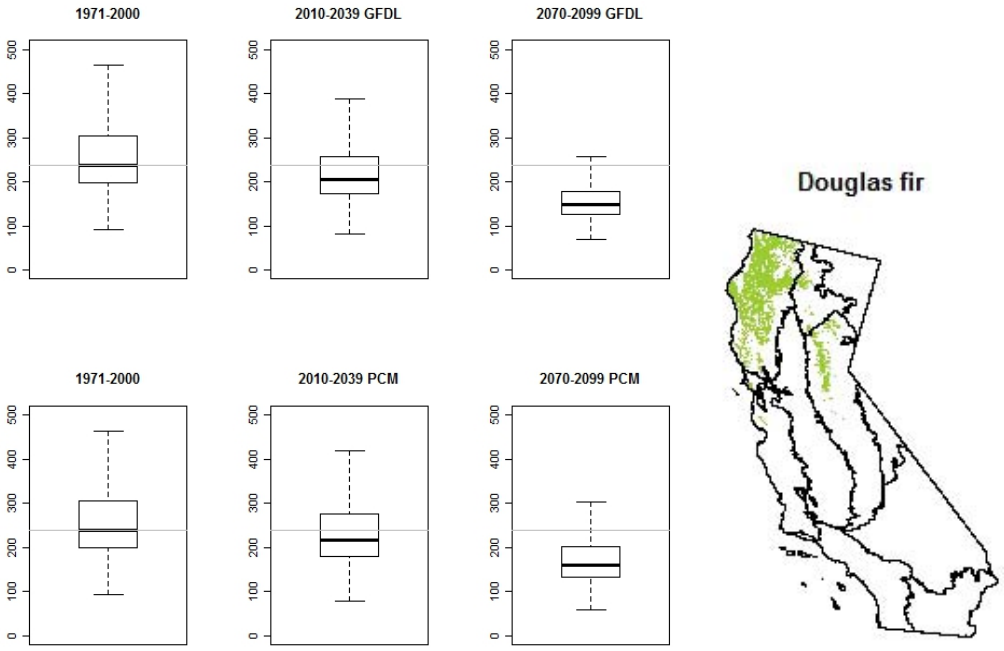
1971-2000
2010-2039 GFDL
2070-2099 GFDL
1971-2000
2010-2039 PCM
2070-2099 PCM
Douglas fir

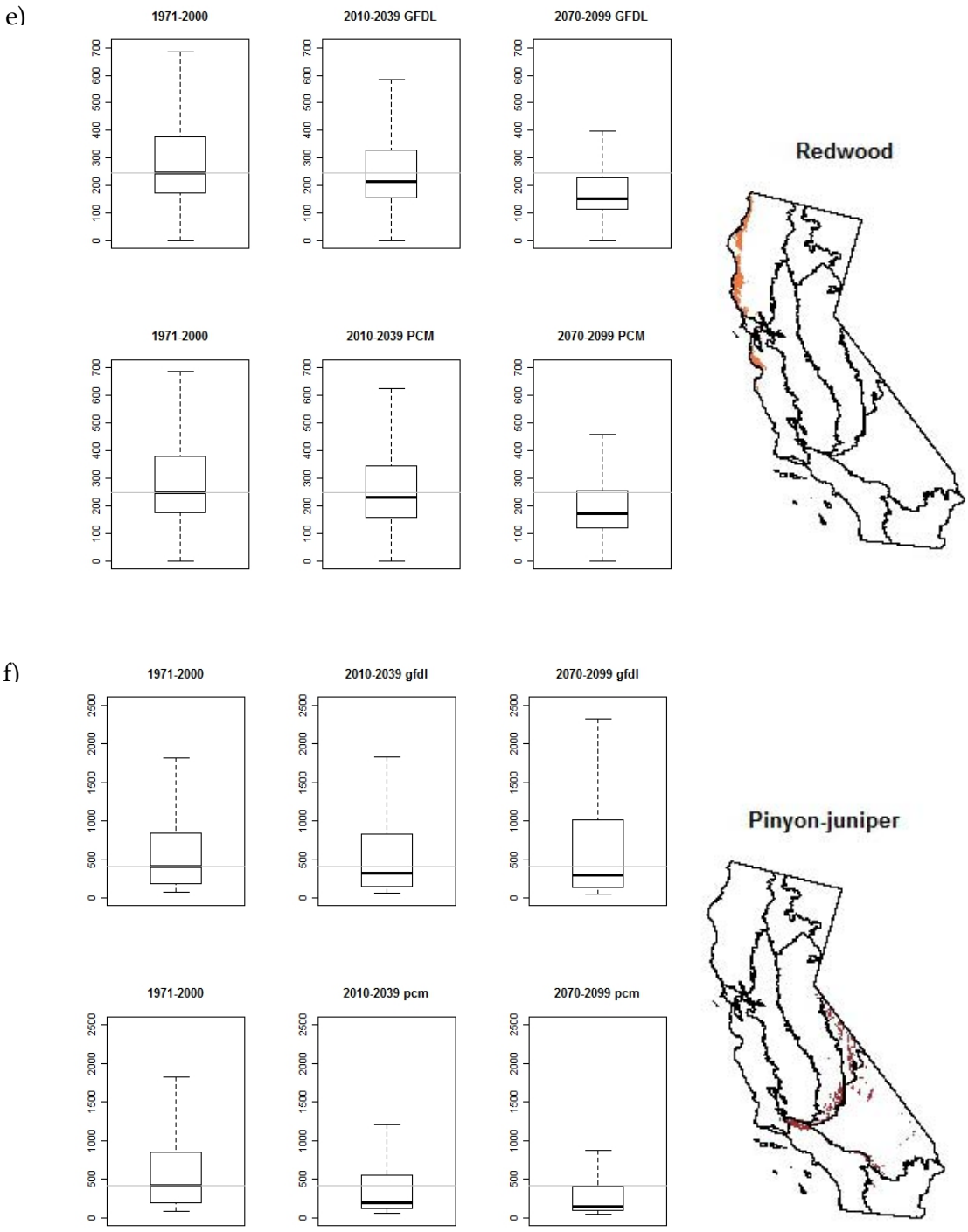

Figure 18: Box and Whisker Plots of Mean Fire Return Interval, mFRI for 1971–2000, 2010–2039, and 2070–2099 Based on GFDL and PCM GCMs for Six Types of Wildlife Habitat Relationship (WHR), (a) Chamise-redshank, (b) Blue oak, (c) Mixed chaparral, (d) Douglas fir, (e) Redwood, and (f) Pinyon-juniper. Note, outliers are not shown. The spatial distribution of each WHR is shown alongside the distributions of return interval.

We mapped the mFRI for landscapes across all of California then focused on the distributions of mFRI for recent historical and future climates for six vegetation types. The mFRI estimates generated here are longer than one might expect for particular vegetation types, especially in Southwestern California. The minimum mFRI among all types was typically around 50 years, found predominantly in the Southwestern California and Central Western ecoregions. It is important to recognize these mFRI values are the mean of expected values for landscapes experiencing a given set of climate conditions. As described in greater detail in Results 1.3.3, random deviates, or draws, from the statistical models would result in a distribution of counts being predicted for each landscape, according to the mean value presented in our maps. In essence, the observed fire counts from which the models were built, and observed fire frequency of particular landscapes we refer to when we identify places on a map, are equivalent to draws—simply one value from a distribution of fire counts, given the mean dynamics of the system.

Changes in the mean frequency of fire varied across the State. In general, large changes in mFRI can be seen by 2070-2099 under both the GFDL and PCM models, but relatively moderate ones for 2010–2039, as would be expected given the same trend in the probabilities of at least one fire and two or more fires. While the statewide maps of mFRI are useful, focus on the changes in the distribution of mFRI for particular vegetation types allows a clearer view of potential future ecological effects of fire~climate relationships. For the six WHR types selected in the study, the general pattern is more frequent fire, indicated by a reduction in the median value of mFRI. The interquartile length is more variable, with some types showing more of a reduced fire frequency, such as the Blue oak and Pinyon-juniper types at 2070–2099 under the GFDL. Not surprisingly, there were some WHR types with larger differences between changes projected for the GFDL and PCM than others—in particular, Blue oak and Pinyon-juniper (2070–2099). The largest changes in mFRI were found within the current geographic range of the Douglas fir WHR type, with a median of mFRI dropping by almost 100 years by 2070–2099. Monitoring the Californian vegetation in burned areas will be a key to understanding how fire and climate change will affect the ecosystems of the region.

Section 2: Fire and Past Climates in California: Back-Casting through the Century

2.1 Introduction

In Section 2, we expand our macro-scaled perspective of fire and climate for California and examine two topics based on back-casted fire projections from our baseline 1971–2000 models presented in Section 1.

First, we provide a preliminary external validation of our baseline 1971–2000 model using a test of temporal transferability. This test was completed by back-casting the probability of fire from the baseline 1971–2000 model parameters while incorporating climate and development data from 1941–1970. These back-casts were compared against model outcomes developed using fire, climate, and development data from the 30-year period from 1941–1970. Though fire records from before 1950 were not kept as reliably as those of more recent periods, this method aids in understanding how well our projections of future fire might reflect actual future events. We

identify areas where models do quite well, and those where there is less agreement. The goal here is not to produce a model that predicts specific historic fire events, but rather to estimate a statewide surface of the expected probability of fire that is the generating function of particular observed events.

Second, we used parameters from the baseline models with observed climate records for periods 1911–1940 and 1941–1970 to make back-casts of fire frequency for those periods. Historical back-projections of human development are represented by housing counts back to 1911. These fire back-casts are interesting because they allow us to ask two important questions. One, if we make the assumption that current human behaviours regarding fire use have remained the same, what might the fire climate and potential fire frequency have been across California earlier in the twentieth century? The notion of invariant human fire-related behaviour is unlikely to hold true, but framing this question allows us to consider how changes in climate might have affected fire environments in the past. We can then ask, are future projections of fire and climate well beyond, or within, the range we might have seen in the last century? We examine how our estimated fire climate has changed over the last century and compare these historical periods to future projections for 2010–2039 and 2070–2099.

2.2 Methods

2.2.1 Fire Data

As described in Section 1, fire data from the California Department of Forestry (CAL FIRE) and Fire Protection Fire and Resource Assessment Program (FRAP) fire polygon dataset[3] were used to develop baseline (1971–2000) statistical models. For Section 2, data from 1941–1970 were also extracted and processed to 1080 m landscapes (Figure 19). Reliability of fire data decreases in the 1941-1970 period due to changes in recording practices, but exploratory analysis of the abundance and distribution of records suggests they were sufficient to proceed with a somewhat heuristic comparative study focused on temporal transferability. Data for the 1911–1940 period is in Figure 19 for comparison but is by no means a complete record of fire.

2.2.2 Climate Data

Climate data were used to represent conditions and resources conducive to fire. As described in Section 1, at the 30-year resolution used for this study, these environmental characteristics include climatological normals rather than specific temporal patterns such as antecedent drought, or fire weather conditions such as a high wind day. Data were provided for all watersheds draining into California at a spatial resolution of 270 m as 30-year averages for each month of the year. These data were generated from historical observations based on PRISM (Daly et al. 2004) data for 1971-2000, 1941-1970, and 1911-1940. In the development of the statistical models we ask, what are the long-term environmental characteristics that lead to landscapes having more or less fire?

2.2.3 Human Development Data

Distance to development was used as a metric of isolation to test for a relationship between landscape fire frequency and human activity, as described in Section 1. Here, we followed the same rationale, yet used the historical development data for model building and back-casting.

[3] CAL FIRE/FRAP. Data. http://frap.fire.ca.gov/data/frapgisdata/select.asp.

The extent and type of development was characterized from data provided by the statewide map of historical housing development by decade, based on the 2000 Census and Department of Finance countrywide projections (http://frap.cdf.ca.gov/data/ frapgismaps/download.asp). The data are based on mapping historic and current housing counts identified in the 2000 U.S. Census of Population and Housing, with developed areas defined as those with a density of one or more housing units per 20 acres. In this dataset, back-casts of development are generated based on the attribute describing the year a structure was built. We aggregated these development indices to match the decades 1911–1940, 1941–1970, and 1971–2000 and sampled them at a resolution of 1080 m. The footprint of these development data for 1971–2000 largely match the UPlan baseline footprint and ICLUS 2000 data categories one through six, as described in Section 1. Euclidean distance quantified the distance to development for every landscape in the study area. We produced a measure of development extent to be used as a mask indicating areas of infrastructure. This was used for mapping, but not in statistical analyses.

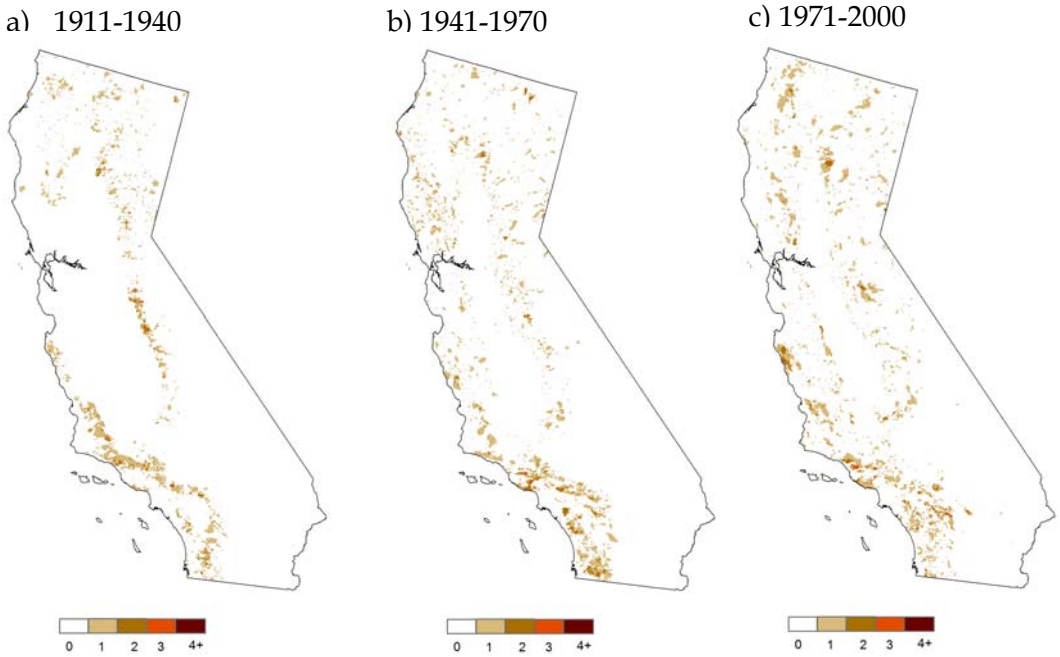

Figure 19: Frequency of Burning in 1080-m Landscapes over 30-year Periods across California in Different Time Intervals, Based on FRAP Data. (a) 1911–1940, (b) 1941–1970, (c) 1971–2000. Note the relative sparseness of data recorded for the 1911–1940 period, reflecting differences in recording.

2.2.4 Land Cover Data

As in Section 1, we used the multi-source land cover product from FRAP, fveg06_1 (http://frap.fire.ca.gov/) to identify water bodies. The original FRAP data were provided at a 30 m resolution, and we aggregated these to 1080 m, based on the modal value of each landscape. The WHR 10-level coding was used to identify water, wetlands, and agricultural areas.

2.2.5 Statistical Modelling

We used statistical models of the relationship between fire counts and explanatory variables for the 30-year recent historical period from 1971–2000, and developed models for 1941–1970, following the same methods as those described in Section 1.

2.2.5.1 Model Development and Assessment

Models for 1971-2000 were the same as those developed in Section 1, and those estimated for 1941–1970 data used the same variables and model forms—i.e., followed the same strategy.

2.2.6 Model Back-Casts

The 10 models of landscape burning built using random samples of the 1971–2000 fire, climate, and urban infrastructure data were used for back-casts. Parameters from these baseline models were used with historical climate and development data to back-cast probability and frequency of landscape fire. Back-casts were generated for situations characterizing 1911–1940 and 1941–1970. Eco-cultural use of fire has changed over the twentieth century, and likely has affected patterns of area burned and fire frequency. The back-casts illustrate the pattern of burning that might have occurred if human behavior toward ignition and suppression mimicked the current time period, yet under the control of historical climates.

Back-casts generated from baseline 1971–2000 model parameters, with 1941–1970 climate and development data were compared against models estimated specifically for 1941–1970.

2.3 Results and Discussion

2.3.1 Model Transferability

The back-cast probability of burning at least once in 1941–1970 (Figure 20) using the baseline 1971–2000 model, hereafter referred to as *baseline back-cast,* shows relatively little overall change as a result of climate and development during the period. Figure 20b illustrates patchy increases and decreases in fire, all within the range of +/- 0.05, where negative values indicate increases in fire and negative values indicate a decrease. The estimated values for the probability of at least one fire appear very similar at first glance for the baseline back-cast versus values estimated from data for 1941–1970, hereafter referred to as *1941–1970 estimates* (Figure 21). However, a test of temporal transferability based on differencing the two values, 1941–1970 estimates minus baseline back-cast, highlights two key areas of difference (Figure 22).

Figure 22a illustrates the delta between the 1941–1970 estimates and baseline back-casts with areas of relatively little change (+/- 0.025) masked in white. There is more fire predicted by baseline back-casts than observed than in 1941–1970 estimates for much of northern and central California and less fire in the southwest. We proposed that potential under-recording of fire for the 1941–1970 period could lead to an overall underestimate of the probability of at least one fire in the 1941–1970 estimates, in contrast to the baseline back-casts, shown in Figure 22. Accordingly, we masked an additional -0.025 from the difference calculations to heuristically account for this potential difference in recording. The result, Figure 22b, shows that while temporal transferability appears to be good for the majority of the region, there are two dominant and spatially clustered areas of difference between the 1941–1970 estimates and baseline back-casts. Based on the climatic and development environment for 1941–1970, the baseline back-casts predicted much more fire around the Central Valley than was estimated from the 1941–1970 records. This trend could be a result of human activities differing from the

baseline period, such as increased farming, grazing, and/or fire suppression leading to reduced fire in these environments in in the 1940s, 50s, and 60s.

In contrast, the baseline back-casts suggest less fire in southwestern California than was expected from the 1941–1970 estimates indicating there was more fire in this region historically than current climate-human interactions would predict. We propose that differences in land management and fire use might be responsible for these outliers. The region is much more urban dominated now than it was earlier in the 1950s and 1960s, and we did not mask out a development footprint for these comparisons. Despite the devastating fires experienced in this area over the last decade, fire might have been more common in some parts of this region in the past, without the urban footprint and suppression activities we see today. Further research is needed to examine historical fire management and cultural use of fire in these two highlighted regions of California.

2.3.2 Historical Back-Casts of Fire and Climate in the Context of Future Projections

The back-casts of fire from the baseline 1971–2000 models for 1911–1940 (Figure 23) and 1941–1970 (Figure 20) climate and development based on baseline 1971–2000 model parameters show patches of altered fire frequency. The largest changes are visible in the 1911–1940 back-cast. Increases in fire, shown by negative values in the delta product, appear in all of the ecoregions, and fire-climate relationships have varied spatially over the twentieth century, leading to increased and decreased likelihoods of burning. Figure 24 shows the full suite of estimates of the mean fire return interval, mFRI, for historical, baseline, and future climate and development scenarios, allowing a comparison of potential future conditions against those experienced in the past. Overall, there appears to be relatively little variability or change in mFRI among the 1911–1940, 1941–1970, and 1971–2000 estimates relative to those projected for 2070–2099. The projections for 2010–2039 seem moderately different from the historical back-casts, with higher frequency of fire most notable in the southwest. Interestingly, the projections for the Mojave and Sonoran desert regions in 2010–2039 under the PCM GCM (warmer-wetter) appear very similar to the patterns back-cast for 1911–1940. In general, projections for 2070–2099 suggest an increasingly short mFRI for most of western California and the Sierra Nevada, well beyond what has been experienced in the past, and consistently projected between both the PCM and GFDL GCMs. Future work integrating model outcomes with fire history studies of these regions would provide useful context for our analyses.

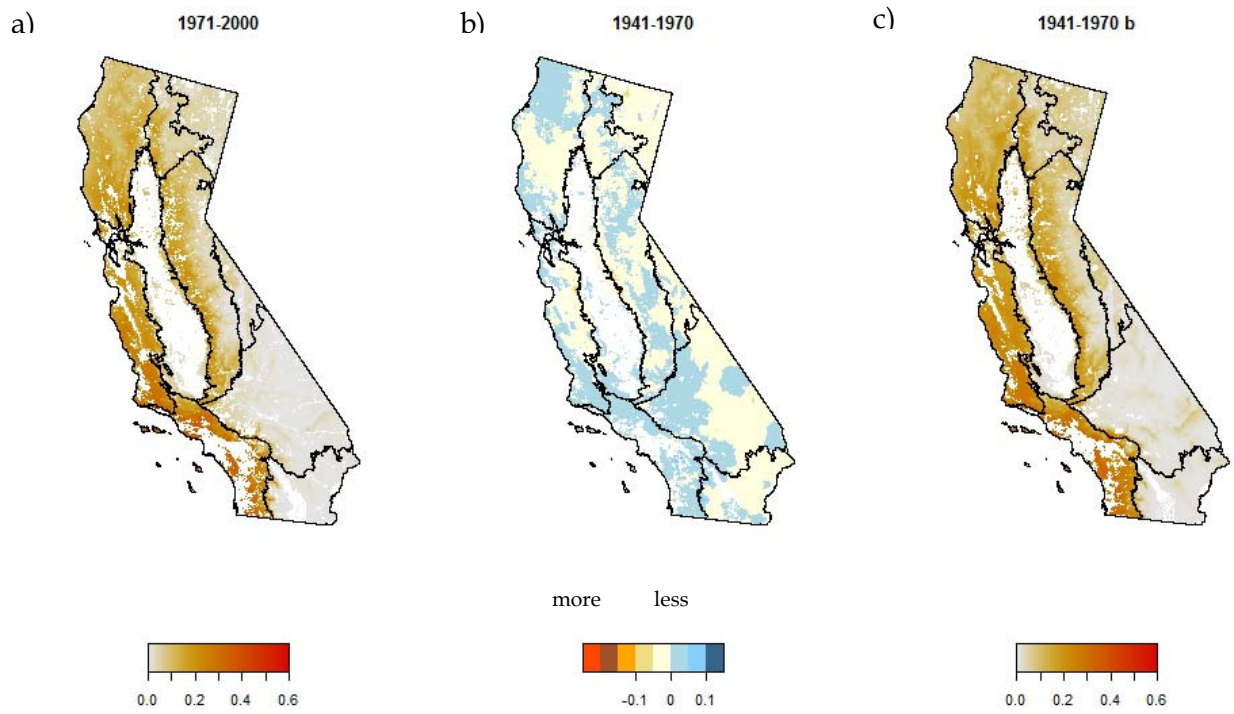

Figure 20: Probability of Burning at Least Once in (a) 1971–2000, (b) the Delta, and (c) the Baseline Back-cast Estimate for 1941–1970 Using 1971–2000 Model Parameters. Delta values represent the baseline 1971–2000 minus the back-cast so that the negative values, indicated by yellow, indicate more fire and positive values, indicated by blue, indicate less fire. Areas in white are masks for development, agriculture, and water.

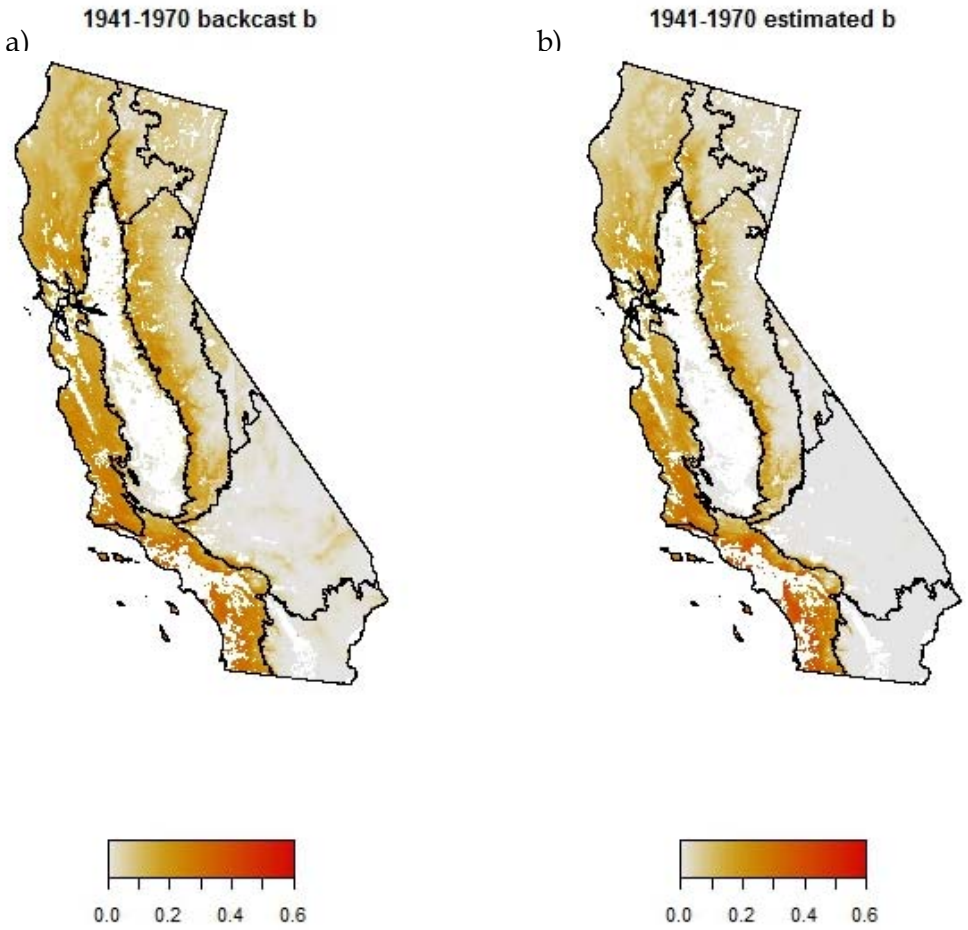

Figure 21: Comparison of Models for Landscapes Burning at Least Once (a) Baseline Back-cast Built with 1971–2000 Data, to (b) 1941–1970 Estimates Built with 1941–1970 Fire Data. Areas in white are masks for development, agriculture, and water.

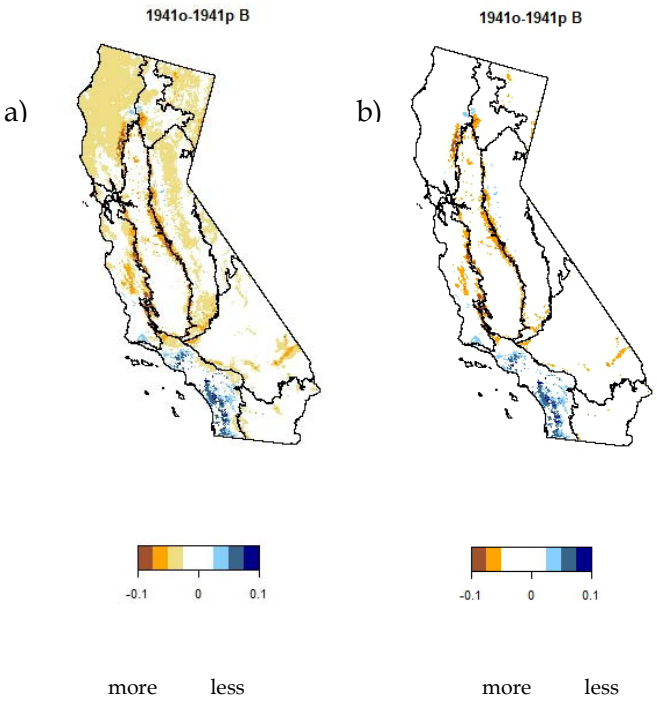

Figure 22: (a) Differences Between 1941–1970 Estimates and Baseline Back-casts. Yellow/orange indicates areas where more fire was predicted by baseline back-casts than in 1941–1970 estimates, blues indicate the reverse. Values are masked to highlight areas of most difference. For (a) the white mask covers areas of little difference, values +/- 0.025. For (b) since general under-reporting might have resulted in an overall diminished probability of fire in the 1941–1970 estimates, the same data are shown but with an additional mask for values up to -0.05. The result highlights key areas of difference between baseline back-casts and 1941–1970 estimates. Areas of agriculture, water, and development at 1941–1970 are also masked in white.

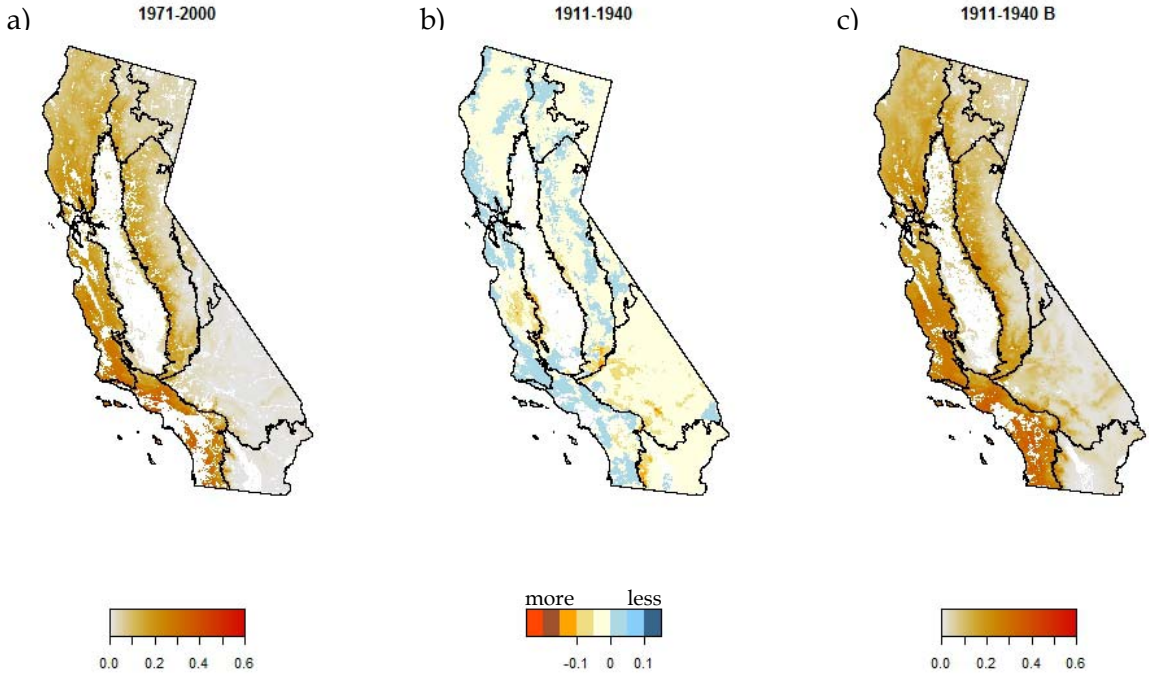

Figure 23: Probability of Burning at Least Once in (a) 1971–2000, (b) the Delta Showing a Subtraction of 1971–2000 Minus 1911–1940 Values, and (c) the Back-cast Estimate for 1911–1940 Based on Baseline 1971–2000 Model Parameters. Areas in white are masks for agriculture (based on 1971–2000 data), development, and water. Note the marked reduction of the development footprint in the southwest.

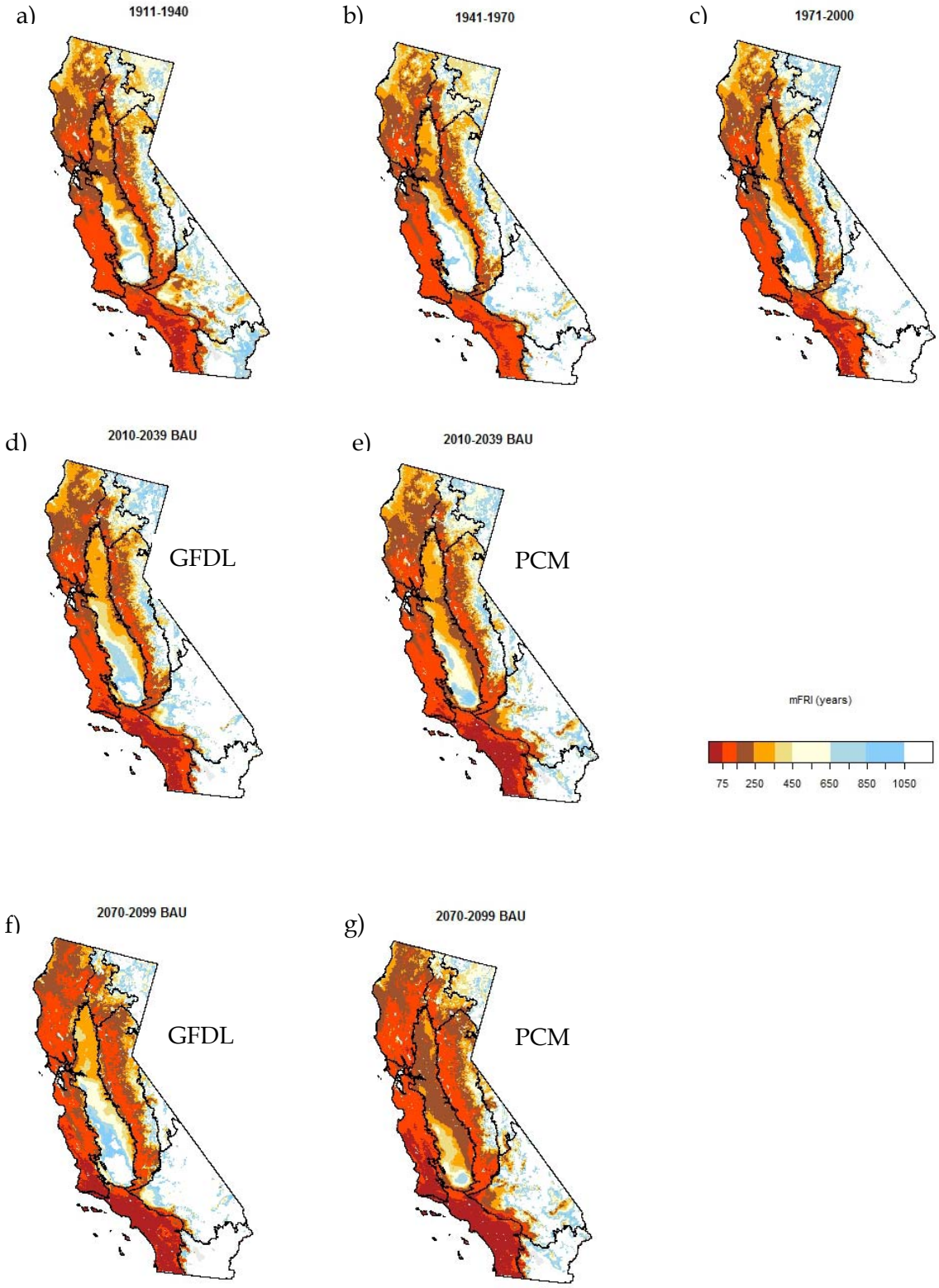

Figure 24: Expected Mean Fire Return Interval (mFRI) for (a) 1911–1940, (b) 1941–1970, (c) 1971–2000, (d,e) 2010–2039 (GFDL then PCM), (f,g) 2070–2099 (GFDL then PCM) Based on 1971–2000 Model Parameters, with no Mask for Agriculture or Development. Water bodies are masked in white.

References

Adam, J. C., and Lettenmaier D. P. 2003. "Adjustment of global gridded precipitation for systematic bias." *Journal of Geophysical Research Atmospheres* 108: 4257, doi: 10.1029/2002JD002499.

Cayan, D. R., Maurer, E. P., Dettinger, M. D., Tyree, M., and Hayhoe, K. 2008. "Climate change scenarios for the California region." *Climatic Change* 87 (s1): S21–S42.

Daly, C., Gibson, W. P., Doggett, M., Smith, J., and Taylor, G. 2004. Up-to-date monthly climate maps for the conterminous United States. Proceedings of the 14th American Meteorological Society Conference on Applied Climatology, American Meteorological Society.

Flint, A. L., and Flint, L. E. 2007. Application of the Basin Characterization Model to estimate in-place recharge and runoff potential in the Basin and Range carbonate-rock aquifer system, White Pine County, Nevada, and adjacent areas in Nevada and Utah. USGS Scientific Investigations Report 2007-5099. 20 p.

Flint, L. E., and Flint, A. L. 2012. "Downscaling future climate scenarios to fine scales for hydrologic and ecological modeling and analysis." *Ecological Processes* 1:1 http://www.ecologicalprocesses.com/1/1/2.

Fulé, P. Z., Ramo-Gomez, M., Cortes-Montano, C., and Miller, A. M. 2011. "Fire regime in a Mexican forest under indigenous resource management." *Ecological Applications* 21: 764–775.

Gedalof, Z., Peterson, D. L., and Mantua, N. J. 2005. "Atmospheric, climatic, and ecological controls on extreme wildfire years in the northwestern United States." *Ecological Applications* 15:154–174.

Hidalgo, H. G., Dettinger, M. D., and Cayan, D. R. 2008. *Downscaling with constructed analogues: 13 daily precipitation and temperature fields over the United States.* California Energy Commission Report. CEC-500-2007-123.

Hoeting, J. A., Davis, R. A., Merton, A. A., and Thompson, S. E. 2006. "Model selection for geostatistical models." *Ecological Applications* 16:87–98.

Hollander, A. D. 2007. California Augmented Multisource Landcover Map V1. Information Center for the Environment, University of California, Davis.

Johnson, D. 1980. "The comparison of usage and availability measurements for evaluating resource preference." *Ecology* 61:65–71.

Keeley, J. E. 2005. *Fire as a threat to biodiversity in fire-type shrublands.* USDA Forest Service General Technical Report PSW-GTR-195. 97 p.

Krawchuk, M. A., and Moritz, M. A. 2011. "Constraints on global fire activity vary across a resource gradient." *Ecology* 92:121–132.

Krawchuk, M. A., Moritz, M. A., Parisien, M. A, Van Dorn, J., and Hayhoe, K. 2009. "Global pyrogeography: The current and future distribution of wildfire." *PLoS ONE* 4:e5102.

Lambert, D. 1992. "Zero-inflated Poisson regression, with an application to defects manufacturing." *Technometrics* 34:1–14.

Littell, J., McKenzie, D., Peterson, D., and Westerling, A. 2009. "Climate and wildfire area burned in western US ecoprovinces, 1916–2003." *Ecological Applications* 19:1003–1021.

Marlon, J. R., Bartlein, P. J., Carcaillet, C., et al. 2008. "Climate and human influences on global biomass burning over the past two millennia." *Nature Geoscience* 1:697–702.

Maurer, E. P., Adam, J. C., and Wood, A. W. 2009. "Climate model based consensus on the hydrologic impacts of climate change to the Rio Lempa basin of Central America." *Hydrological and Earth System Science* 13:183–194.

McKelvey, K. S., Skinner, C. N., Chang, C. et al. 1996. An overview of fire in the Sierra Nevada. Pages 1033–1040 *In* Anonymous Sierra Nevada Ecosystem Project: Final report to Congress, vol. II, University of California, Centers for Water and Wildland Resources, Davis.

Meehl G. A., Covey C., Delworth T., et al. 2007. "The WCRP CMIP3 multimodel dataset: A new era in climate change research." *Bulletin of the American Meteorological Society* 88: 1383–1394.

Moritz, M. A., Parisien, M-A., Batllori, E., Krawchuk, M. A., VanDorn, J., Ganz, D. J., and Hayhoe, K. Climate change and disruptions to global fire activity. In review: *Ecosphere*.

Meyn, A., White, P. S., Buhk, C., and Jentsch, A. 2007. "Environmental drivers of large, infrequent wildfires: The emerging conceptual model." *Progress in Physical Geography* 31:287–312.

Nakicenovic N., et al. 2000. *IPCC special report on emissions scenarios.* Cambridge, U.K.: Cambridge University Press.

National Research Council. 2011. *Climate stabilization targets: Emissions, concentrations, and impacts over decades to millennia.* Washington, D.C.: National Academies Press.

Parisien, M. A., Snetsinger, S., Greenberg, J. A. et al. 2012. "Spatial variability in wildfire probability across the western United States." *International Journal of Wildland Fire*, Online first.

Parisien, M. A., and Moritz, M. A. 2009. "Environmental controls on the distribution of wildfire at multiple spatial scales." *Ecological Monographs* 79:127–154.

Pausas, J. G., and Keeley, J. E. 2009. "A Burning Story: The Role of Fire in the History of Life." *BioScience* 59:593–601.

Pechony, O., and Shindell, D. T. 2010. "Driving forces of global wildfires over the past millennium and the forthcoming century." *Proceedings of the National Academy of Sciences* 107:19167–19170.

Power M., J. Marlon, N. Ortiz, et al. 2008. "Changes in fire regimes since the Last Glacial Maximum: An assessment based on a global synthesis and analysis of charcoal data." *Climate Dynamics* 30:887–907.

Scholze, M., Knorr, W., Arnell, N. W., and Prentice, I. C. 2006. "A climate-change risk analysis for world ecosystems." *Proceedings of the National Academy of Sciences* 103:13116–13120.

Stephenson, N. L. 1998. "Actual evapotranspiration and deficit: Biologically meaningful correlates of vegetation distribution across spatial scales." *Journal of Biogeography* 25:855–870.

Swetnam, T. W., and Betancourt, J. L. 1990. "Fire - Southern Oscillation Relations in the Southwestern United-States." *Science* 249:1017–1020.

Syphard, A. D., Radeloff, V. C., Keeley, J. E., et al. 2007. "Human influence on California fire regimes." *Ecological Applications* 17:1388–1402.

Theobald, D. M. 2005. "Landscape patterns of exurban growth in the USA from 1980 to 2020." *Ecology and Society* 10:32. [online] URL: http://ecologyandsociety.org/vol10/iss1/art32/.

van der Werf, G. R., Randerson, J. T., Giglio, L., et al. 2008. "Climate controls on the variability of fires in the tropics and subtropics." *Global Biogeochemical Cycles* 22: GB30328.

Vogelmann, J. E., Howard, S. M., Yang, et al. 2001. "Completion of the 1990s National Land Cover Data Set for the Conterminous United States from Landsat Thematic Mapper Data and Ancillary Data Sources." *Photogrammetric Engineering and Remote Sensing* 67:650–662.

Walker, W. T., Gao, S., and Johnston, R. A. 2007. "UPlan: Geographic information system as framework for integrated land use planning model." *Transportation Research Record* 1994:117–127.

Waller, E. K., Parisien, M.-A., Krawchuk, M. A., and Moritz, M. A. 2007. Quantifying expected area burned for carbon accounting protocols. White paper. University of California, Berkeley. 24 pp.

Westerling, A. L., Bryant, B. P., Preisler, H. K., Holmes, T.P., Hidalgo, H., Das, T., and Shrestha, S.. 2011. "Climatic change and growth scenarios for California wildfire." *Climatic Change* 109(s1): 445–463.

Westerling, A., and Bryant, B. P. 2008. "Climate change and wildfire in California." *Climatic Change* 87:231–249.

Westerling, A. L., Hidalgo, H. G., Cayan, D. R., and Swetnam, T. W. 2006. "Warming and earlier spring increase western US forest wildfire activity." *Science* 313:940–943.

Westerling, A. L., Gershunov, A., Brown, T. J., Cayan, D. R., and Dettinger, M. D. 2003. "Climate and wildfire in the western United States." *Bulletin of the American Meteorological Society* 84:595–604.

Wood, A. W., Leung, L. R., Sridhar, V., and Lettenmaier, D. P. 2004. "Hydrologic implications of dynamical and statistical approaches to downscaling climate model outputs." *Climatic Change* 62:189–216.

Whitlock, C., Higuera, P. E., McWethy, D. B., and Briles, C. E. 2010. "Paleoecological perspectives on fire ecology: Revisiting the fire-regime concept." *The Open Ecology Journal* 3: 6–23.

Zuur, A. F. 2009. Zero-truncated and zero-inflated models for count data. Pages 261-293 *In* Mixed effects models and extensions in ecology with R, Springer Science and Business Media.

Glossary

AIC	Akaike Information Criterion
BCM	Basin Characterization Model
BLM	Bureau of Land Management
CAL FIRE (CDF)	California Department of Forestry and Fire Protection
CMIP3	Coupled Model Intercomparison Project phase 3
FRAP	Fire and Resource Assessment Program
GCM	Global Climate Model
ICLUS	Integrated Climate and Land-use Scenarios
IPCC	Intergovernmental Panel on Climate Change
mFRI	mean Fire Return Interval
NCAR PCM	National Center for Atmospheric Research Parallel Climate Model
NOAA GFDL CM2.1	National Oceanic and Atmospheric Administration's Geophysical Fluid Dynamics Laboratory Climate Model 2.1
PIER	Public Interest Energy Research
PRISM	Parameter-elevation Regressions on Independent Slopes Model
SRES	Special Report on Emission Scenarios
USDA	United States Department of Agriculture
WCRP	World Climate Research Programme
WHR	Wildlife Habitat Relationship type
ZIP	Zero-inflated Poisson